INORGANIC CHEMISTRY
FRONTIERS

REVIEW

View Article Online
View Journal | View Issue

Cite this: *Inorg. Chem. Front.*, 2020, **7**, 1822

Enabling high performance n-type metal oxide semiconductors at low temperatures for thin film transistors

Nidhi Tiwari, [a] Amoolya Nirmal,[b] Mohit Rameshchandra Kulkarni,[b] Rohit Abraham John [b] and Nripan Mathews *[a,b]

Amorphous oxide semiconductors have drawn considerable attention as a replacement for ubiquitous silicon based technologies. By virtue of their flexible substrate compatibility and transparency, amorphous metal oxide semiconductor (AOS) thin film transistors (TFTs) are being explored in emerging flexible/transparent technologies. However, rapid advances in such technologies require the development of high-performance thin film transistors, which can be fabricated at low processing temperatures. In this review paper, we discuss the recent progress made in n-type semiconductor TFTs activated at low temperatures both on rigid and flexible substrates with a focus on the replacement of conventional high temperature annealing. Several low temperature processing approaches that have been reported in both vacuum deposited and solution processed n-type metal oxide semiconductor based thin film transistors are evaluated, with an emphasis on some novel techniques which can effectively modulate the electronic properties of the n-type metal oxide semiconductor systems at low temperatures. The final part of this review draws conclusions and discusses the outlook for future research efforts in achieving low temperature activated high performance n-type TFTs.

Received 12th January 2020,
Accepted 8th March 2020

DOI: 10.1039/d0qi00038h

rsc.li/frontiers-inorganic

1. Introduction

Thin-film transistors (TFTs) have been the focus of intense worldwide research during the past decade, and have emerged as fundamental building blocks for optoelectronic devices such as flat-panel displays, liquid crystal displays (LCDs) and active matrix organic light emitting diodes (AMOLEDs),

[a]*Energy Research Institute @ NTU (ERI@N), Nanyang Technological University, Singapore 637553*
[b]*School of Materials Science and Engineering, Nanyang Technological University, 50 Nanyang Avenue, Singapore 639798. E-mail: Nripan@ntu.edu.sg*

Nidhi Tiwari

Nidhi Tiwari is a Postdoctoral Research Fellow in the Energy Research Institute at Nanyang Technological University, Singapore since 2017. She received her Ph.D. from the National Chiao Tung University, Taiwan in 2016. Her research focuses on flexible and transparent oxide-based semiconductors in context to applications in thin film transistors, and neuromorphic and photovoltaic electronic devices.

Amoolya Nirmal

Amoolya Nirmal is a Postdoctoral Research Fellow at the School of Materials Science and Engineering, Nanyang Technological University, Singapore. She received her M. Sc. from the National University of Singapore and her PhD in Electrical and Electronics Engineering in 2017 from Nanyang Technological University. Her current research focus is on solution processable metal oxide semiconductors and dielectrics and 2D composites for thin film transistor applications.

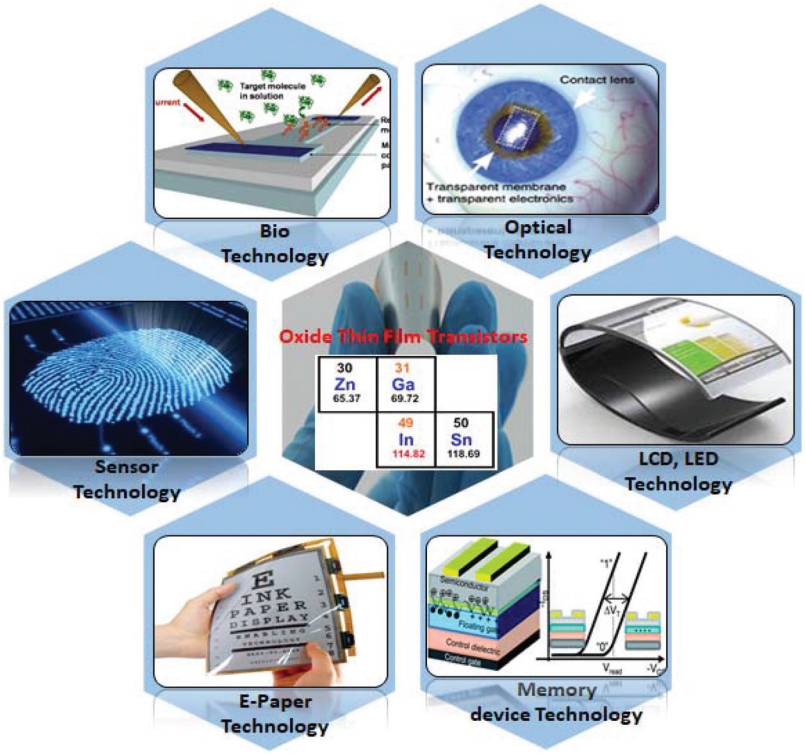

Fig. 1 Metal oxides for thin film transistors and their applications in flexible electronics.

wherein they perform a critical function in display operation.[1–5] With the display technology's insatiable demand for higher resolution, larger screen size, lower power consumption and reduced costs, a-Si thin-film transistors have been challenged by low-temperature polycrystalline silicon and metal–oxide TFTs. In comparison with low-temperature poly-Si (LTPS) TFTs, metal oxide TFTs present inherent advantages such as improved large-area uniformity and considerably lower manufacturing cost, while maintaining high carrier mobility, good transparency and reasonable electrical reliability/stability.[6,7] By virtue of their flexible substrate compatibility and transparency, amorphous metal oxide semiconductor (AOS) TFTs are of interest in emergent technologies such as flexible displays, flexible transparent circuitry, electronic skin, smart contact lenses and flexible neuromorphic devices (Fig. 1).[8,9] Metal oxide (MO) semiconductors contain heavy post-transition metal cations with $(n-1)\,d^{10}ns^0$ $(n \geq 5)$ electronic configurations, where the large radii of the metal ns

Mohit Rameshchandra Kulkarni

Kulkarni Mohit Rameshchandra is a Postdoctoral Research Fellow at the School of Materials Science and Engineering, Nanyang Technological University, Singapore. He received his Ph.D. from Nanyang Technological University, Singapore under the supervision of Prof. Nripan Mathews. His research focuses on flexible transparent electronics focusing on oxide semiconductors, thin film transistors, pressure–strain–temperature sensors, mechanical energy harvesting, and neuromorphic electronic devices.

Rohit Abraham John

Rohit Abraham John received his Ph.D. degree from Nanyang Technological University in 2019 under the supervision of Prof. Nripan Mathews. Currently, he works as a Research Fellow in the same lab focussing on neuromorphic electronic devices, oxide semiconductors, thin film transistors and memory devices.

orbitals lead to adjacent orbital overlap and consequently result in a high degree of wave-function overlap, electron delocalization, and relatively high electron mobility, independent of the microstructure. As a result, they retain relatively high electron mobility even in the amorphous state, thus making them an ideal material for high throughput and low cost manufacturing processes.[10] Deposition of these thin films is achieved by using either vacuum techniques such as sputtering, atomic layer deposition (ALD) *etc*. or ambient pressure solution-processed TFTs requiring relatively higher processing temperatures (temperature >350 °C) for optimum film formation, densification, and impurity removal. Oxide semiconductor thin films formed at low temperatures exhibit poor electrical characteristics due to the presence of numerous defects and impurities and the high temperature post-deposition annealing aids in modulating their electronic properties for the fabrication of high performance thin film transistors.[3,6] Recently significant effort has been expended to explore new materials compositions and novel processing methodologies to improve the electronic transport in metal oxides, and to lower the processing temperature for compatibility with low-cost and flexible polymer substrate materials.[8] New alternatives for activation/improvement of the properties of oxide thin film transistors are also being concurrently explored, with the research focus currently leaning towards oxygen vacancy modulation of MO semiconductors.[3,8] Metal oxide semiconductors for thin film transistors have been reviewed previously.[3,8,11,12] Among these, majority of the reviews that focus on low temperature processing dealt with solution processed metal oxide systems. In this review, we discuss low temperature fabrication of metal oxide TFTs (≤300 °C) using both solution and vacuum processing. In addition to reviewing the prevalent low temperature methods such as photoactivation, microwave and combustion synthesis *etc*. which have been reviewed previously,[3,8,11,12] we also explore and analyze more unconventional athermal methods such as capping layer and electric field driven approaches which have been recently reported to result in high performance devices.

Electronic structure modulation: In 1996, Hosono *et al.* proposed a multicomponent combination of cations for the design of an amorphous metal oxide semiconductor. The selected cations possess conduction bands derived from large ionic-radius, spherically symmetric 4s, 5s, or 6s electron orbitals from the portion of the periodic table shown in the inset of Fig. 1. Since then, there have been many metal oxide semiconductor trials with the most prevalent ones involving indium (In), tin (Sn), zinc (Zn), and gallium (Ga) as AOS design starting points. This is because their binary oxides such as indium oxide (In_2O_3), tin-oxide (SnO_2), and zinc oxide (ZnO) are the three most commonly used transparent conducting oxides (TCOs).[13] These materials have wide band gaps (E_g > 3 eV), high transparency (>80%) and high electrical conductivity. Additionally, they retain relatively high electron mobility even in the amorphous state and are hence widely considered as the base materials for amorphous MO semiconductors. The small effective masses and corresponding relatively high mobility of these oxides are valued for both TCO and AOS applications. However, these materials suffer from very high carrier concentrations, non-uniformity and high leakage currents. These issues were addressed by mixing two or more metal cations to form ternary or quaternary systems, to boost the formation of amorphous films, thereby reducing the carrier concentration and decreasing the grain boundaries present in polycrystalline samples.[10] For MO TFTs to exhibit a low I_{off}, high I_{on} and stable performance, it is imperative to limit the semiconductor carrier concentration to a low level, preferably $<10^{17}$ cm^{-3}.[10,14] In the case of binary or ternary MO systems, moderate n-type doping can be controlled by the cation/anion non-stoichiometry or process optimization. An alternative approach is to introduce an extra component, such as a carrier suppressor (a dopant). The primary requirements for dopants are the following: (i) M–O bond strength should be higher than that of the matrix metal ion; (ii) dopant size should be smaller than the matrix host metal ion size; else the dopant will act as a defect site;[15] (iii) high Lewis acid strength, since it results in higher mobility *via* suppression of scattering by oxygen interstitials;[16] and (iv) an appropriate concentration of the dopant to ensure accurate control of the oxygen vacancies without a significant decrease in the mobility. Various elements such as gallium (Ga), tungsten (W), silicon (Si), hafnium (Hf), zirconium (Zr), titanium (Ti), aluminum (Al) and tantalum (Ta) have been studied and shown to exhibit carrier suppressor behavior.[16] Therefore, the cation composition can be modified to improve the stability of transparent metal oxide (TMO) TFTs under bias and illumination stress. In addition, incorporation of nitrogen into the binary systems also appears to suppress the growth of indium oxide and zinc oxide resulting in a nanostructured phase.[14] The substitution of an oxygen anion with a nitrogen anion effectively passivates the V_O sites in ZnO and In_2O_3 by eliminating the oxygen deficiency related deep levels near the

Nripan Mathews

Nripan Mathews is an Associate Professor and Provost's Chair in Materials Science and Engineering at the School of Materials Science and Engineering at Nanyang Technological University (NTU), Singapore. He obtained his first degree in Materials Engineering from NTU and his MSc under the Singapore-MIT alliance. Following his Ph.D. at Paris VI University, he was also a Visiting Scientist at École Polytechnique Fédérale de Lausanne (EPFL). Nripan's interest lies in the development of novel and inexpensive electronic materials through cost-effective techniques for electronics and energy conversion. These include organic–inorganic halide perovskites, metal oxides, and organic thin films.

valence band maximum, thereby improving the photo-bias stability.[14,17]

Processing methods: Electronic and optoelectronic devices based on metal oxides usually comprise thin films deposited on appropriate substrates. High-quality metal oxide networks can be obtained by using extremely controlled deposition processes such as pulsed laser deposition (PLD) and atomic layer deposition (ALD) and even by using less sophisticated methods such as radiofrequency (RF) magnetron sputtering as depicted in Fig. 2a–c. These techniques permit the growth of high-quality uniform thin films with atomic layer precision.[18] Solution processing is another widely adopted method for fabricating MO films for TFT applications and is appealing in terms of its low cost, scalability and compatibility with high throughput manufacturing. Fig. 2d illustrates the stages involved in solution processing, namely, the synthesis of the solution, deposition of the solution on substrates and pyrolysis or condensation for MO formation. The evolution of the film as it proceeds through these stages is also illustrated. The various deposition techniques employed, such as spin-coating, inkjet printing and spray coating, are presented in Fig. 2e. The nanoparticle route and precursor route are two widely adopted approaches for the synthesis of the solution for metal oxide film formation. The nanoparticle route is a straightforward approach wherein a metal oxide nanoparticle dispersion in appropriate solvent is deposited on the substrate. The evolution of metal oxide films deposited through the precursor route is depicted in Fig. 2f, where the metal cation complexes formed by the solvation of metal precursors undergo hydrolysis and condensation reactions to form a metal–oxide (M–O) network. Although the nanoparticle approach seems advantageous in terms of low temperature processing, the inherent

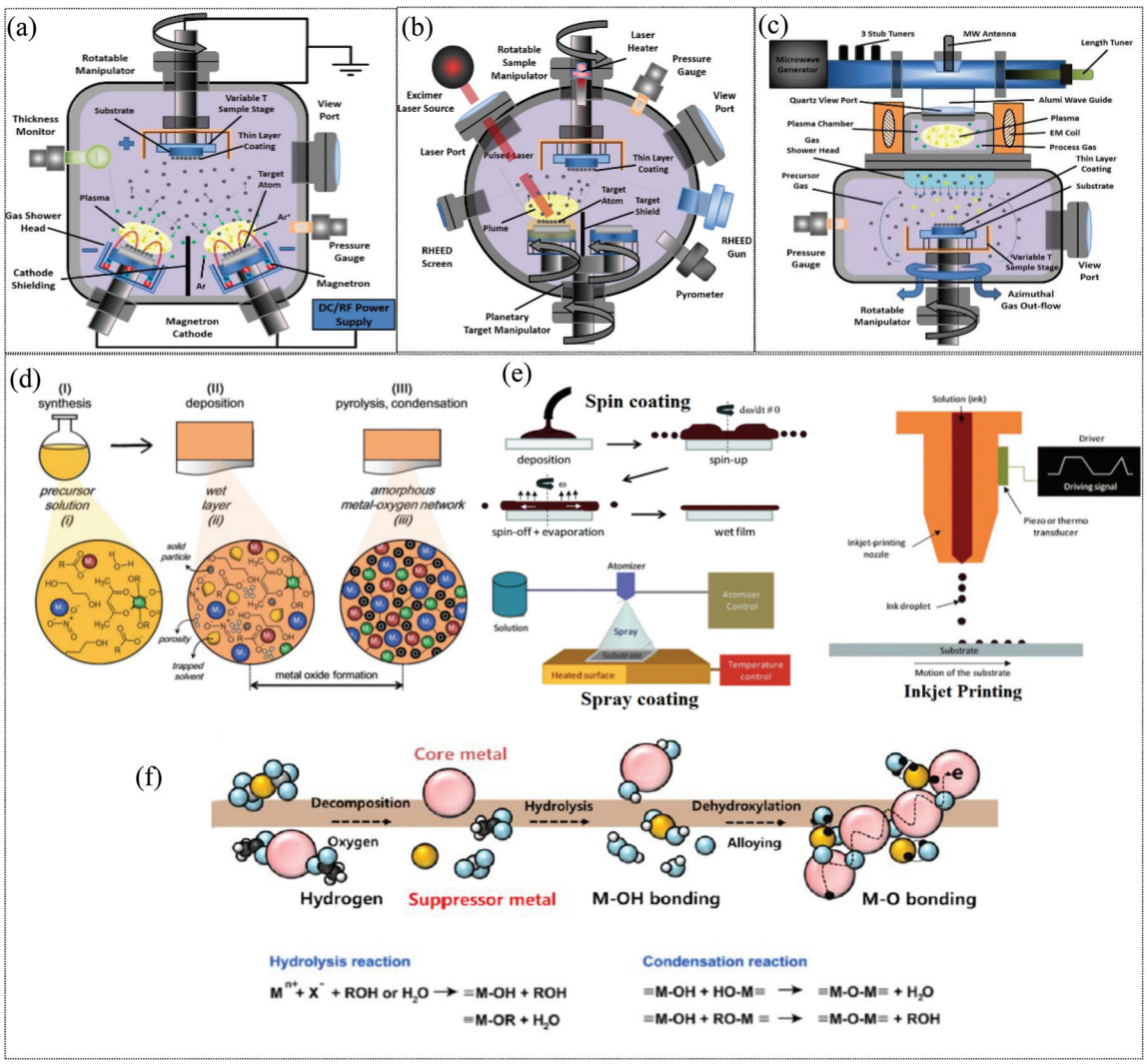

Fig. 2 Low-cost deposition techniques used to produce electronic devices based on semiconducting metal oxides. (a) RF magnetron sputtering, (b) pulsed laser deposition (PLD), (c) atomic layer deposition (ALD) (reproduced from ref. 18), (d) stages of solution processing of metal oxide films (reproduced from ref. 168), (e) deposition techniques (reproduced from ref. 168), and (f) a schematic of the evolution of metal oxide films through precursor route film deposition and subsequent annealing (reproduced from ref. 21).

porous nature affects the film quality and the particle boundaries limit charge transport which severely impair the device characteristics of the fabricated TFTs.[19–21] In comparison, the precursor route aids in the formation of denser, grain boundary-free MO films with lower surface roughness. However, it needs to be noted that high temperature annealing is generally a prerequisite for the formation of high-quality metal oxide films for effective and complete hydrolysis, condensation and densification reactions which are imperative for the formation of M–O–M networks and for the removal of organic residues.

Table 1 summarizes the recent progress made on n-type metal oxide TFTs processed at temperatures below 300 °C. The table lists a selection of MO TFTs fabricated on rigid substrates, which is further divided into TFTs that use a SiO_2 dielectric and those employing high-*k* dielectrics. The table also lists a selection of MO TFTs fabricated on flexible substrates. The technique used for MO film formation and the processing and post-processing annealing temperatures (where applicable) are listed for each, together with the important figures of merit of TFT performance (the mobility and on/off ratio). The materials are listed in the order of binary, ternary and quaternary metal oxide systems with the TFT reports. In general, the following observations can be made: (i) mobilities above 10 can be achieved in metal oxide TFTs even at low processing temperatures, (ii) TFT performance is more robust on rigid substrates when compared to those on flexible substrates, (ii) vacuum processed metal oxide films are superior in quality and hence lead to overall enhanced device characteristics and (iv) high-*k* dielectrics with their higher gate capacitance and interface quality result in devices with high mobility at low operation voltages.

2. Low-temperature route for n-type metal oxide semiconductors

Previous studies have proven that MO films annealed at high temperature (>400 °C) exhibited good TFT device characteristics. However, low-temperature processing (≤350 °C) is indispensable for realizing AOS TFTs for flexible electronic applications and a low thermal budget post-deposition annealing (PDA) process is required to minimize the production cost. In this context, conventional thermal annealing (CTA), which has been generally adopted for the PDA process, is disadvantageous in terms of the duration and high thermal budget required. Herein we discuss the various approaches reported, broadly divided into physical and chemical routes to reduce the processing temperature for the fabrication of metal oxide based TFTs.

2.1 Physical routes for the reduction of process temperature

2.1.1 High pressure annealing. High pressure annealing (HPA), has been recently reported as a promising alternative to CTA for the formation of high-quality metal oxide films. HPA is effective in the activation of sputtered films, as in the case of IGZO reported by Kim *et al.*[110] The mechanism of activation by employing N_2 and O_2 high pressure activation is illustrated in Fig. 3a. Here, the temperature necessary for activation was reduced from 300 to 100 °C with the incorporation of HPA in N_2 and O_2 gases, where the kinetic energy of the gas molecules provides the activation energy required, while the incorporation of O_2 gas provides the additional benefit of elevating the metal oxide construction by ensuring sufficient ns metal orbital overlap for efficient charge transport while simultaneously reducing the electron trap density at lower pressure as is evident in Fig. 3b. This results in TFTs with higher bias stress stability and higher mobility (~11 $cm^2 V^{-1} s^{-1}$) at a low temperature of 100 °C compared to TFTs annealed at 300 °C. In the case of solution processed metal oxide films, HPA requires lower fabrication temperature compared to CTA methods as it reduces the Gibbs free energy and decomposition temperature for the formation of the metal oxide network, with minimal organic residues.[111] In addition, employing HPA also produces denser MO films due to the drastic reduction of porosity, a bane, especially for low temperature solution processed MO films (Fig. 3). Definitive work on HPA annealing has been done by Kim *et al.* and in 2012 they demonstrated a solution processed IZO TFT on a polyimide (PI) substrate subjected to 1 MPa HPA under an O_2 atmosphere at 220 °C.[112] The reduced bulk defects and charge traps provided by HPA also resulted in more stable devices as indicated by the positive bias stress with the lowest V_{th} shift obtained for 1 MPa O_2 HPA. In addition to activation, HPA can also be utilized as a post-treatment for activated films, as the process can assist in improving the electrical stability of TFTs through defect passivation and enhanced densification of metal oxide films. However, HPA requires a long duration of treatment (~1 h) and a specialized O_2/N_2 environment under high pressure conditions which could hamper widespread industrial applications. Though promising as a CTA replacement, the scalability issues of utilizing HPA for metal oxide layer activation for TFT applications need to be addressed as a facile integration of this activation method into a roll-to-roll production process flow will be challenging.

2.1.2 Microwave annealing approach. The microwave assisted annealing (MWA) technique has attracted significant attention due to the volumetric heating involved, which directly and uniformly delivers thermal energy to the MO film, while enabling a low thermal budget and fast processing, primarily due to the short exposure duration.[70,113–117] In principle, microwaves compromise with rapid changes in electric and magnetic fields as well (Fig. 4a). The microwave will heat any material with mobile electric charges such as ions in dielectrics. For example, polar solvents are heated due to the interaction of the time varying fields with the polar molecules. As a result, the polar molecules tend to vibrate with the fields and lose energy in collisions. Charges such as ions or electrons within the semiconducting and conducting materials constitute the electric current in response to the field and the resulting loss in energy through resistive heating and dielectric relaxation of the materials. In particular, the resistive heating/ohmic loss dominates at lower frequencies (<10 GHz). Thus

Table 1 n-Type TFTs processed at low temperature

Material	Technique	($T_{dep.}$/$T_{post.}$)/(°C)	Substrate	Dielectric	Mobility ($cm^2 V^{-1} s^{-1}$)	On/off ratio	
Metal oxide TFTs on rigid substrates							
In_2O_3	Evaporation	200	Silicon	SiO_2	27	10^4	22
IZO	Sputtering	—	Glass	SiO_x	157	10^{10}	23
IWO	Sputtering	150	Silicon	SiO_2	39	10^{10}	24
IWO	Sputtering	100	Silicon	SiO_2	36.7	10^7	25
IWO	Sputtering	100	Silicon	SiO_2	27.55	10^8	26
IWO/IWO:N	Sputtering	100	Silicon	SiO_2	27.2	10^7	27
IWZO	Sputtering	300	Silicon	SiO_2	22.30	10^8	28
IZTO	ALD	180/350	Silicon	SiO_2	27.8	10^{11}	29
IGZO	ALD	—/250	Silicon	SiO_2	22.1	10^8	30
IGZO	Sputtering	300/240	Silicon	SiO_2	14.72	10^9	31
IGZO	Sputtering	150/new	Silicon	SiO_2	12.68	10^8	32
IGZO	Sputtering	RT/350	Silicon	SiO_2	11.2	10^8	33
IGZO	Sputtering	RT/300	Silicon	SiO_2	9.21		34
AIZO	Sputtering	225	Silicon	SiO_2	20.65	10^7	35
AIZO	Sputtering	RT	Glass	SiO_2	5.67	10^6	36
ITO/ATZO	Sputtering	—	Glass	SiO_2	246	10^8	37
ZNON	Sputtering	Light irradiation	Silicon	SiO_2	48.4	10^9	38
InON	Sputtering	300	Silicon	SiO_2	9.55	10^7	17
SnO_2	Sputtering	180	Silicon	HfO_2	92	10^6	39
In_2O_3	ALD	300	Glass	Al_2O_3	41.8	10^7	40
In_2O_3	ALD	160/300	Silicon	Al_2O_3	7.8	10^7	41
ZnO	ALD	—/200	Silicon	Al_2O_3	27.8	10^9	42
IZO	Sputtering	300	Glass	SiN_x/p-SiO_x	50.4	10^{10}	43
IZO/HIZO	Sputtering	250	Glass	SiN_x/SiO_x	48.28	10^7	44
PrIZO	Sputtering	300	Glass	SiO_2/Si_3N_4	26.3	10^8	45
IZO/IZO:Si	Sputtering	300	silicon	SiO_2	15.30	10^8	46
IZO/ZnO/IGZO	Sputtering	300	silicon	SiO_2	14.0	10^8	47
ITO	Sputtering	200	Glass	Al_2O_3	56.1	10^9	48
ITO	Sputtering	250	Glass	Al_2O_3	25.9	10^9	49
IGO	ALD	200/300	Glass	Al_2O_3	9.45	10^8	50
IGO	Sputtering	RT	Glass	Al_2O_3	2.66	10^6	51
IGZO	Sputtering	RT/200	Silicon	HfO_2	38.29	10^6	52
IGZO	Sputtering	RT/100	Silicon	SiN_x	26.03	10^7	53
IGZO	Sputtering	70	Silicon	Al_2O_3	6.3	10^7	54
IGZO	Sputtering	RT	Glass	Al_xO_y	5.4	10^6	55
IGTO	Sputtering	150	Glass	PVP-*co*-PMMA, PMF, HfO_x	25.9	10^7	56
HIZO	Sputtering	300	Glass	SiN_x/SiO_2	13.73	10^{12}	57
IZO/IGZO	Spin-coating	—/300	Si	Al_2O_3	25	10^7	58
In_2O_3	Spin-coating	—/250	Si	SiO_2	23.53	10^6	59
Ni-InO	Spin-coating	—/350	Si	SiO_2	17.71	10^6	60
Metal oxide TFTs on flexible substrates							
ZnO	ALD	100/—	PET	Al_2O_3	37.1	10^7	61
ZnO	PEALD	200/—	PI	Al_2O_3	12	10^8	62
ZnO	Sputtering	RT/RT	PEN	Al_2O_3	11.56	10^8	63
ZnO	Sputtering	100/—	PET	HfO_2	7.95	10^8	64
ZnO	Hydrothermal	90/100	PET	PMMA	7.53	10^4	65
ZnO	Spin-coating	—/160	PEN	Al_2O_3-ZrO_2	5	10^4	66
ZnO	ALD	150/—	PI	Al_2O_3	3.07	10^2	67
ZnO	Printing	—/250	PI	Ion-gel	1.67	10^5	68
ZnO	Sputtering	—/225	PI	HfO_2	1.6	10^6	69
ZnO	Sputtering	—/MW	PES	Al_2O_3	1.5	10^6	70
ZnO	Sputtering	RT/350	PDMS	SiO_2	1.3	10^6	71
ZnO	Spin-coating	RT/200	PI	SiO_2	0.35	10^6	72
ZnO	Spin-coating	—/150	PES	Hybrid	0.142	10^4	73
ZnO	Spin-coating	—/200	PET	c-PVP	0.09	10^5	74
ZnO	Spin-coating	—/135	PEN	RSiO1.5	0.07	10^4	75
ZTO	Inkjet-print	30/300	PI	ZrO_2	0.04	10^3	76
IZO	Sputtering	RT/RT	PET	SiO_2	65.8	10^6	77
IZO	Spin-coating	RT/280	PI	Zr-Al_2O_3	51	10^4	78
IZO	Sputtering	—/300	PI	Al_2O_3	6.64	10^7	79
IZO	SCS	275/—	Polyester	Al_2O_3/ZrO_2	3.9/6.2	10^4	80
IZO	Spin-coating	RT/350	PI	K-PIB	4.1	10^5	81
IZO:F	Spin-coating	RT/200	PEN	Al_2O_3	4.1	10^8	15
IWO	Sputtering	270	PI	Al_2O_3	25.86	10^5	82
ZITO	PLD	RT/—	PET	v-SAND	110	10^4	83
ZITO	Sputtering	300/200	PI	SiO_2	32.9	10^9	84
ZITO	Sputtering	RT/—	Polyarylate	Al_2O_3	16.93	10^9	85
IGZO	Spin-coating	RT/350	PI	Al_2O_3	84.4	10^5	86

Table 1 *(Contd.)*

Metal oxide TFTs on rigid substrates

Material	Technique	($T_{dep.}$/$T_{post.}$)/(°C)	Substrate	Dielectric	Mobility (cm^2 V^{-1} s^{-1})	On/off ratio	
IGZO	Sputtering	RT/RT	PC	$SiO_2/TiO_2/SiO_2$	76	10^5	87
IGZO	Sputtering	RT/200	PI	HfLaO	22.1	10^5	88
IGZO	Sputtering	RT/200	PDMS	P(VDF-TrFE)	21	10^7	89
IGZO	Sputtering	200/220	PI	SiO_2	19.6	10^9	90
IGZO	Sputtering	RT/—	PI	Al_2O_3	17	10^5	91
IGZO	Sputtering	RT/180	PEN	Al_2O_3	15.5	10^9	92
IGZO	Sputtering	—/180	PEN	Si_3N_4	13	10^8	93
IGZO	Sputtering	150/150	PEN	Al_2O_3	12.87	10^9	94
IGZO	Sputtering	—/160	PEN	Al_2O_3	11.2	10^9	95
IGZO	Spin-coating	—/PN254 nm	PI	ZAO	11	10^9	96
IGZO	Sputtering	RT/110	PET	c-PVP	10.2	10^6	97
IGZO	Sputtering	RT/150	PVA	SiO_2/Si_3N_4	10	10^6	98
IGZO	Sputtering	—/300	Thin glass	Si_3N_4	9.1	10^8	99
IGZO	Sputtering	RT/190	PEN	SiO_2	8	10^7	100
IGZO	Sputtering	—/PN254 nm	PAR	Al_2O_3	7	10^8	101
IGZO	Spin-coating	—/PN254 nm	PI	Al_2O_3	5.41	10^8	102
IGZO	Sputtering	RT/—	PI	Al_2O_3/SiO_2	4.93	5	103
IGZO	Sputtering	RT/—	PI	PVP	3.6	10^4	104
IGZO	Sputtering	RT/—	PEN	PVP	0.43	10^5	105
IGZO	Sputtering	RT/200	PDMS	P(VDF-TrFE)	0.35	10^4	106
IGZO/IZO	Sputtering	40/200	PEN	SiO_2	18	10^9	107
IGZO	Spin-coating	—/140 200	PI	Al_2O_3	1.5	10^4	108
In_2O_3	Flexographic printing	—/200	PI	Al_2O_3	2.83	10^6	109

the MWA process has been shown to provide a lower temperature process that results in good activation.[118] In 2010, T. Jun *et al.* demonstrated a comparison between hot plate annealing and microwave annealing effects on the performance of a solution processed ZnO TFT. Microwave-annealing of ZnO TFTs on a rigid substrate for 30 min at 140 °C showed a better field effect mobility of 1.7 cm^2 V^{-1} s^{-1} compared to hot plate annealing (0.32 cm^2 V^{-1} s^{-1}). Additionally, transistors on flexible substrates exhibited device characteristics of 0.57 cm^2 V^{-1} s^{-1}. Microwave annealing reduces the grain boundaries due to an increase in the size of the ZnO nanoparticles and leads to improved transport properties of the charge carriers, resulting in better performance of the TFT.[113] In 2014, S. Park *et al.* also investigated the effect of microwave annealing on a sputtered ZnO TFT (Fig. 4b). The microwave irradiation of 2.45 GHz at 700 W for 15 min increased the field effect mobility from 0.2 to 1.5 cm^2 V^{-1} s^{-1} and the on/off current ratio from 36.5 to 6.9 × 10^6. The microwave irradiation induces a large number of oxygen vacancies as confirmed by photoluminescence, resulting in enhanced mobilities.[70] H.-C. Cheng also demonstrated a microwave annealed solution processed flexible a-IZO TFT[119] with a mobility of 6.9 cm^2 V^{-1} s^{-1}, and an I_{ON}/I_{OFF} ratio greater than 10^6 (Fig. 4d). In 2014, Lee *et al.* demonstrated highly reliable microwave assisted annealed a-IGZO thin-film transistors to be used as biosensors. Microwave irradiation of 2.45 GHz at 1000 W for 10 min improved the TFT performance (μ_{FE} = 9.51 cm^2 V^{-1} s^{-1}, V_{th} = 0.99 V, I_{ON}/I_{OFF} = 1.18 × 10^8), compared to that of furnace-annealed a-IGZO TFTs at 400 °C for 30 min (μ_{FE} = 4.51 cm^2 V^{-1} s^{-1}, V_{th} = 4.85 V, I_{ON}/I_{OFF} = 3.38 × 10^7). The microwave annealing eliminated the defect density inside the a-IGZO film and improved the device performance. In addition, the microwave-assisted annealed TFT displayed excellent sensing properties in terms of pH sensitivity, reliability, and chemical stability when employed as a transducer in an extended-gate ion-sensitive field-effect transistor biosensor.[114] In 2015, K.-W. Jo and his co-workers developed ultra-thin (5 nm) SnO_2 TFTs. The performance of the TFTs was significantly improved with a field effect mobility of 35.4 cm^2 V^{-1} s^{-1} and I_{ON}/I_{OFF} = 4.48 × 10^7 under microwave irradiation of 2.45 GHz at 1000 W for 15 min assisted annealing as compared to that of CTA (400 °C, 30 min) TFTs (μ_{FE} = 20.3 cm^2 V^{-1} s^{-1}, I_{ON}/I_{OFF} = 2.76 × 10^7) as depicted in Fig. 4e. This result is due to the enhancement of crystallinity and elimination of defects in SnO_2 TFTs by the microwave irradiation.[115] In 2019, Shin reported the microwave-assisted annealing of various compositional ratios of sputtered IGZO films under O_2 ambient atmosphere (Fig. 4c). The temperature of the a-IGZO TFT samples was measured using an infrared thermometer during the MW-PDA process and observed to be 399.6 °C on average. However, CTA at 400 °C showed poorer performance since MWA results in lowered defect densities (D_{it}, N_t) and subgap density of states (DOS).[116] Compared to conventional annealing techniques, the novel microwave annealing techniques facilitate low temperature activation of devices on flexible substrates and may be promising for roll to roll processing of flexible electronics.[117] In addition, microwave annealing is also more efficient at improving the electrical performance of IGZO TFTs than the other low temperature annealing processes such as electron beam (e-beam) radiation and low-temperature hot-plate annealing. It is shown that, the IGZO TFTs subjected to microwave annealing exhibit a typical field effect mobility of 11.3 cm^2 V^{-1} s^{-1} and a threshold voltage of −1.54 V, while the TFTs subjected to e-beam annealing exhibit a slightly lower mobility of 7.40 cm^2 V^{-1} s^{-1} and a more negative

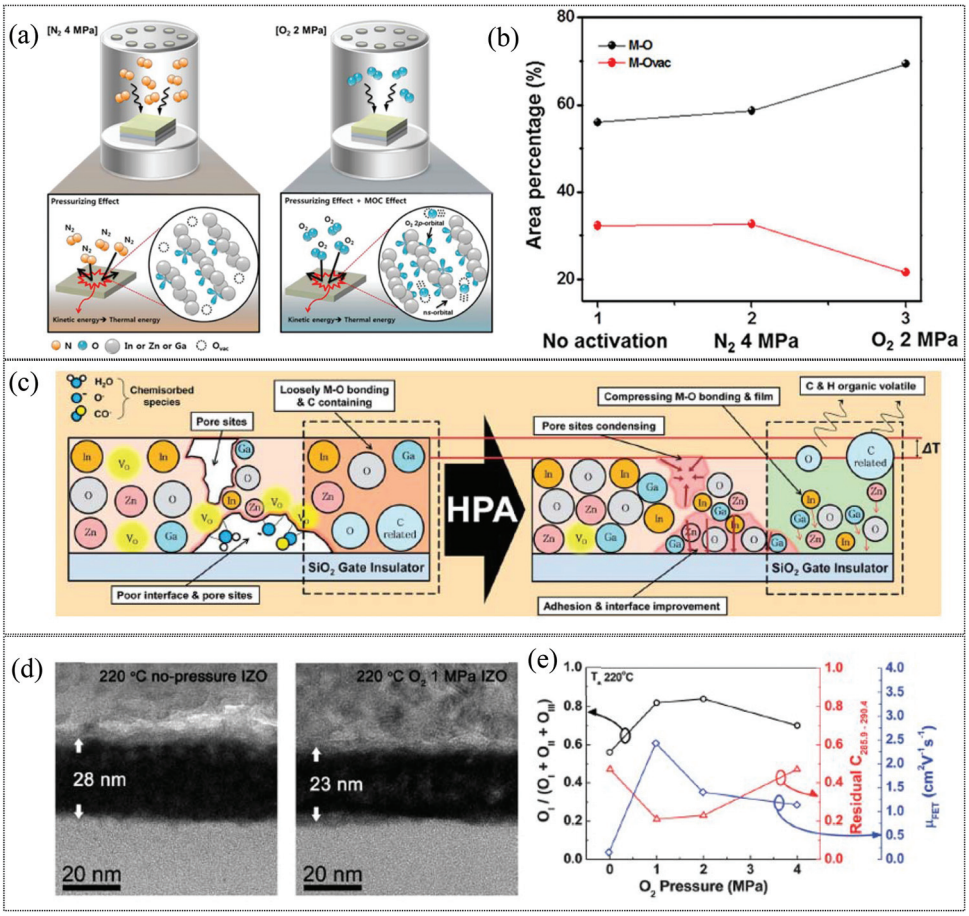

Fig. 3 (a) Schematic of the effect of N_2 and O_2 HPA on sputtered IGZO films (reproduced from ref. 110), (b) area ratio of M–O and M–O_{vac} for various conditions (reproduced from ref. 110), (c) illustration of the effect of high pressure on low temperature solution-processed metal oxide thin films (reproduced from ref. 112), (d) cross-sectional HRTEM image of the IZO thin film annealed at 220 °C (right) and at 220 °C in 1 MPa O_2 (reproduced from ref. 112), and (e) the $O_I/O_I + O_{II} + O_{III}$ ratio, residual carbon ratio (286.1 + 287.1 + 288.1 + 288.9 eV/284.6 eV), and field-effect mobilities as functions of O_2 pressure (reproduced from ref. 112).

threshold voltage of −1.95 V. The poor performance is attributed to structural damage during e-beam radiation, which generates electrical defect levels within the forbidden band gap of IGZO.[120] However, the low-temperature hot-plate annealing resulted in comparable device performance with microwave annealing and both microwave annealing and low-temperature hot-plate annealing increased the mobility from 12.3 $cm^2\ V^{-1}\ s^{-1}$ (as-deposited) to ~19 $cm^2\ V^{-1}\ s^{-1}$ in microwave and hot plate annealing states. However, the negative shift in the threshold voltage with microwave annealing (from 0.23 V to −2.86 V) is smaller than that with low-temperature hotplate annealing (to −9 V) due to the suppression of oxygen vacancy formation.[121] Microwave annealing offers various advantages such as rapid and effective heating, low temperature processing, and suppression of unnecessary diffusion to the adjacent material. However, there may be challenges in terms of safety and variations associated with the specific sample size and the shape may also need to be managed.

2.1.3 Photoactivation. Photoactivation is the most prevalent substitute for thermal annealing of MO films, especially for solution processed MO films, where the light source provides photothermal energy sufficient to initiate the chemical conversion for the formation of metal oxide networks. Photoactivation has been demonstrated with deep UV irradiation as a viable annealing technique for the formation of MO films such as IZO, IGZO and IO. Recently, there have been reports on the use of other sources including infrared and intense pulsed light for the activation of metal oxide films for TFT applications.[122–124] Deep UV (DUV) irradiation provides sufficient energy for the decomposition, condensation and densification reactions and results in MO films with properties comparable to high temperature CTA MO films (mechanism of activation is illustrated in Fig. 5a). In 2012, Park *et al.* demonstrated the use of DUV irradiation, specifically suitable for nitrate precursors (compared to acetate or chloride precursors) by virtue of their stronger absorption of UV irradiation.[125] Though there is inherent heating to around 150 °C during photoactivation, which may aid in the removal of organic residues, this is insufficient as an independent thermal energy source for the formation of M–O–M networks, as is evident in

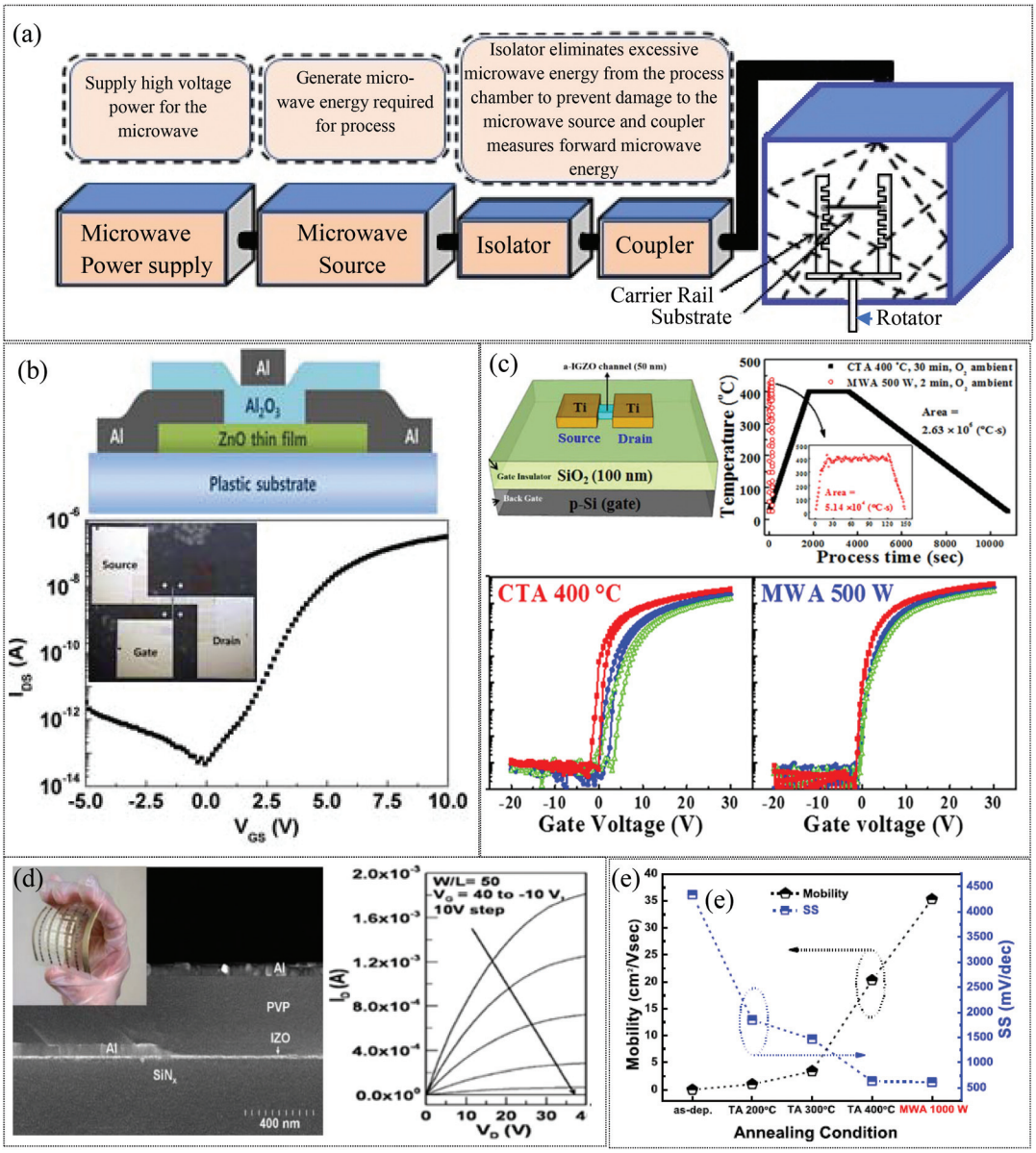

Fig. 4 (a) A schematic of the microwave annealing system (reproduced from ref. 169). (b) A schematic of the flexible ZnO TFT and transfer characteristics of the microwave processed flexible device (reproduced from ref. 70). (c) Schematic diagram of back-gate top-contact structure a-IGZO TFTs, temperature profile of the annealing process using CTA at 400 °C for 30 min in O_2 and MWA at 500 W for 2 min in O_2, respectively, and transfer characteristics of microwave and CTA processed devices (reproduced from ref. 116). (d) SEM local cross-sectional image of the flexible a-IZO TFT device on the PI substrate; the inset shows a flexed 5 cm × 5 cm PI substrate with 27 a-IZO TFT devices and output characteristics (reproduced from ref. 119). (e) Field-effect mobility (μ_{EF}) and subthreshold swing (SS) of 5 nm thick UTB SnO_2 TFTs annealed under different conditions (reproduced from ref. 115).

Fig. 5b. Though initially demonstrated under an inert atmosphere, UV photochemical activation was shown to be equally effective under ambient conditions as reported by Mathews *et al.*[126] Here, a mid-UV range source with emission spectra of 200 to 300 nm, corresponding to 398.48 to 598.2 kJ mol^{-1}, was used to ensure decomposition of precursors and initiate condensation and densification for the formation of high quality InO and IZO films with TFT mobilities of ~30 $cm^2 V^{-1} s^{-1}$. On the other hand, infrared irradiation activation relies on the rapid photothermal effect provided by IR irradiation (Fig. 5c). IR irradiation increases the free energy of the precursor system, elevating it to a metastable state, which reduces the activation energy necessary for the formation of the oxide network. Thus, in comparison with conventional thermal annealing, with adequate duration of IR irradiation, lower temperature is sufficient for complete precursor decomposition and metal oxide network formation. This results in metal oxide films with higher carrier concentration and lower

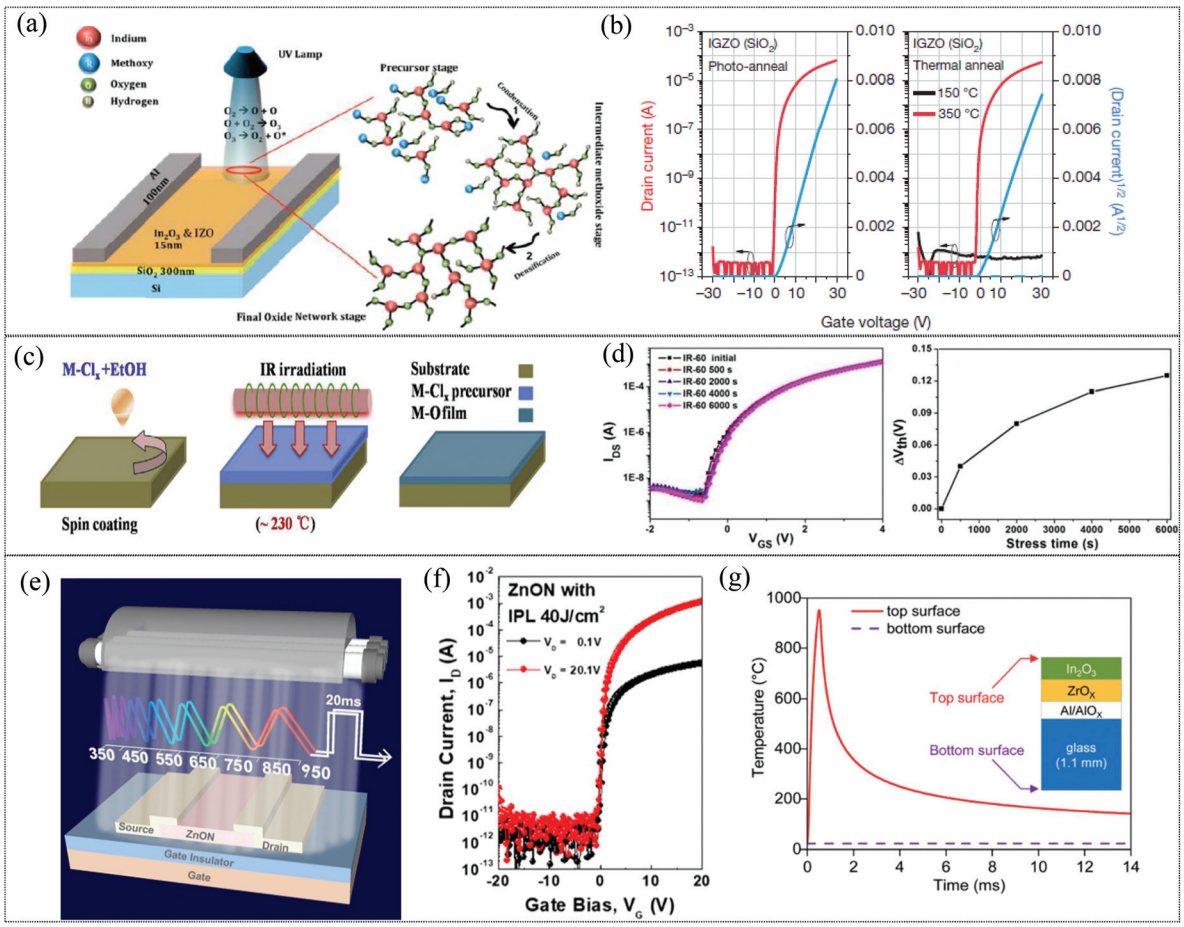

Fig. 5 (a) Proposed mechanism for photochemical activation *via* UV irradiation (reproduced from ref. 126). (b) Transfer and output characteristics of photo-annealed and thermally annealed (150 and 350 °C) IGZO TFTs (reproduced from ref. 125). (c) Process flow of IR irradiation activation for formation of a metal oxide film (reproduced from ref. 123). (d) Transfer characteristics and V_{th} shift results of positive bias stress on IGZO TFTs activated by IR irradiation (reproduced from ref. 122). (e) Illustration of sub-second exposure of IPL (xenon flash lamp) for activation (reproduced from ref. 128). (f) Transfer characteristics of IPL activated ZnON TFTs at different drain voltages (reproduced from ref. 128). (g) Simulation results obtained using the SimPulse software of the temperature at the top and at the bottom of the In_2O_3 TFT fabricated on a 1.1 mm-thick glass substrate after exposure to a xenon light pulse (reproduced from ref. 127).

defect density due to improved interface quality and higher oxygen vacancy generation. Wang *et al.* reported that an IGZO TFT fabricated by IR irradiation (induced temperature of 230 °C) in ambient environments could achieve a mobility of 60 cm^2 V^{-1} s^{-1}, and an I_{ON}/I_{OFF} ratio of 10^6.[122] This was a marked improvement in mobility compared to those of conventional high temperature (450 °C) annealed IGZO TFTs. The higher M–O bond content and oxygen vacancies and lower M–OH content and trap density demonstrated by the IR irradiated MO layers in comparison with thermally annealed counterparts are indicative of a high quality, low defect content metal oxide layer with good interface quality which manifests in the high stability exhibited during a positive bias stress test (Fig. 5d). Unlike UV annealing, IR irradiation is also effective with chloride precursors (which typically require >400 °C annealing). Xia *et al.* have reported the use of IR irradiation to form both an AlO_x solution processed dielectric and an IO film employing chloride precursors.[123] The resultant AlO_x dielectric demonstrated properties comparable to vacuum processed counterparts with a capacitance of 158 nF cm^{-2} and a small leakage current (5.4 Å–10^{-8} A cm^{-2}) by virtue of the low defect density of IR irradiated films. The IO TFTs exhibited a mobility of around 33 cm^2 V^{-1} s^{-1}. However, the incidental temperature on the substrate during IR radiation is higher than that generated during UV irradiation, which may make it unsuitable for certain flexible substrates. The primary advantage of other novel photoactivation sources such as intense pulse light is the sub-second exposure duration necessary for the activation of the metal oxide films which ensures selective heating of the precursor film. Intense pulsed light (IPL) using a xenon light source was used for the photoactivation of solution processed MO films such as IGZO and In_2O_3 TFTs and In_2O_3/ZnO heterojunctions for TFT applications.[124,127] It was also used for the activation of sputtered ZnON films, where a 20 ms pulse of 40 J cm^{-2} resulted in TFT devices with high stress stability and a mobility of around 48 cm^2 V^{-1} s^{-1}.[128] Even though the inci-

dental heating can be as high at 1000 °C during exposure in the case of a xenon flash lamp, the sub-second (500 μs–20 ms) exposure duration ensures negligible heating of the substrate (Fig. 5g).[127] In_2O_3 TFTs were fabricated on polyimide (PI) and heat-stabilized polyethylene naphthalate (PEN) substrates using xenon lamp photonic activation, demonstrating their compatibility with flexible substrates.[129] Thus, photoactivation seems to be a prime candidate for the replacement of CTA, providing a low temperature alternative to form high performance metal oxide films with condensation and densification comparable to those of their high temperature annealed counterparts.[130] In addition, photochemically activated films have been reported to result in improved surface roughness (<0.7 nm or below) compared to CTA samples, which can aid in enhancing device performance.[129] Studies on bias illumination stress behaviors have shown that the photoactivated samples show enhanced stability and faster recovery when compared to CTA samples.[20] In addition, the durations of these photoactivation techniques range from a few ms (in the case of IPL) to a few min to less than an hour (in the case of deep UV and IR), which is beneficial from a high throughput R2R manufacturing point of view. However, it has to be noted that the materials properties of the metal oxide films or precursors such as their absorption range, thermal conductivity *etc*., have a profound effect on the successful photoactivation of the films.[129] In the case of deep UV photoactivation of solution processed films, the nitrate precursors are preferred due to its favorable UV absorption may be harmful due to the NO_x decomposition byproduct. DUV is also known to be incompatible to various flexible substrates and has been shown to reduce the optical transmission of certain flexible substrates.[123] Due to the limitations of the photoactivated area using IPL, the feasibility of scaling up of the activation process for large area or R2R production has to be investigated.

Sections 2.1.1–2.1.3 discussed the widely reported alternatives to CTA. However, there are always unavoidable thermal components in many of these processes and other limitations that make them incompatible with flexible substrates. Recently, there have been studies on other novel physical techniques which effectively modulate the oxygen vacancies/electronic structures of MO films athermally, with an additional advantage of being substrate independent. Among these, the use of capping layers and ionic liquid activation are two promising techniques, which will be covered in the following sections.

2.1.4 Capping layers. In AOS TFTs, electron mobility is sensitive to defect states and therefore the mobility is expected to increase significantly by reducing the defect density. Metallic capping layers overlaid between S/D contacts reduce drain current-crowding and the carrier scattering effect due to their lower value of sheet resistance.[131] Additionally, the proposed devices effectively prevent the adsorption/desorption reaction of ambient oxygen and hydrogen molecules on the surface. This structure showed high μ_{FE} and enhanced stability simply by adopting a metal capping layer.[132] In 2012, H.-W. Zan *et al.* demonstrated an amorphous indium–gallium–zinc oxide (a-IGZO) TFT with a double capping layer of metal calcium/aluminium at its back channel (Fig. 6a). The mobility of the TFT increased from 12 to 160 $cm^2\ V^{-1}\ s^{-1}$ after deposition of the capping layer of Ca/Al. The Ca layer (150 μm long, 35 nm thick) deposited on the back channel of these devices served as the mobility enhancement capping layer, while the Al layer deterred the formation of CaO, $Ca(OH)_2$ and $CaCO_3$ by absorption of oxygen, water and carbon dioxide, respectively, from the atmosphere. The Ca atoms close to the IGZO layer react with weakly bonded oxygen atoms of Zn–O, In–O, and Ga–O to form Ca–O bonds and enhance the field effect mobility of the device due to the reduction of defect density.[132] In 2015, Z. Wang *et al.* successfully demonstrated facile fabrication of a CMOS inverter at low temperature by using single-step deposition of a tin mono-oxide channel layer (Fig. 6b). Selective deposition of a copper oxide capping layer on top of the tin mono-oxide provided additional oxygen to form an n-type SnO_2 phase at temperature as low as 190 °C in air. The phase transition from SnO to SnO_2 typically occurs at temperatures above 300 °C. However, in the case of a bilayer system this can occur at temperatures as low as 190 °C.[133] In 2017, Y. Shin *et al.* showed low-temperature crystallization of IGZO using a tantalum (Ta) catalytic layer. The field-effect mobility was significantly boosted to 54.0 $cm^2\ V^{-1}\ s^{-1}$ for the IGZO device with a metal induced polycrystalline channel formed at 300 °C as compared to 18.1 $cm^2\ V^{-1}\ s^{-1}$ for the non-catalysed IGZO TFT. A 20 nm thick Ta thin film, serving as the crystallization catalytic layer, was sputtered selectively through a shadow mask on top of the active layer between the source and drain electrodes. Improvement in the device mobility occurred because Ta acted as a catalyst to break weak IGZO bonds, and these broken bonds within IGZO rearranged to form crystallized regions during thermal annealing.[134] In 2019, T. Kim and co-workers also investigated novel TaO_x encapsulation to enhance the performance of ZnO:N thin-film transistors (Fig. 6c). A 10 nm thick Ta film was selectively deposited and annealed at 200 °C for 1 h under O_2 ambient atmosphere. Ta capped TFTs (μ_{FE} = 89.4 $cm^2\ V^{-1}\ s^{-1}$, V_{th} = −0.45 V, $I_{ON/OFF}$ = 8.6×10^8) showed improved performance when compared to uncapped TFTs (μ_{FE} = 36.2 $cm^2\ V^{-1}\ s^{-1}$, V_{th} = 1.28 V, $I_{ON/OFF}$ = 2.9×10^8) owing to scavenging and passivation effects of the TaO_x film which occurred due to facile elevation of the quasi-Fermi level as a result of a lower acceptor-like trap state distribution and a large carrier concentration value. A smaller number of sub-gap states near the conduction band (CB) minimum and a higher net carrier density for the TaO_x-capped devices increased the Fermi energy level toward the CB edge under thermal equilibrium conditions, thus leading to efficient band conduction and fast carrier transport under the on-state conditions.[135] Various metal capping layers have been shown to improve device performance and stability; however, the additional patterning steps required for the capping layer increases the manufacturing cost. It also lowers the optical transparency of transparent electronics due to a reduced aperture ratio.[136]

2.1.5 Ionic liquid approach or electric field driven approaches. Owing to the capability to generate an extremely

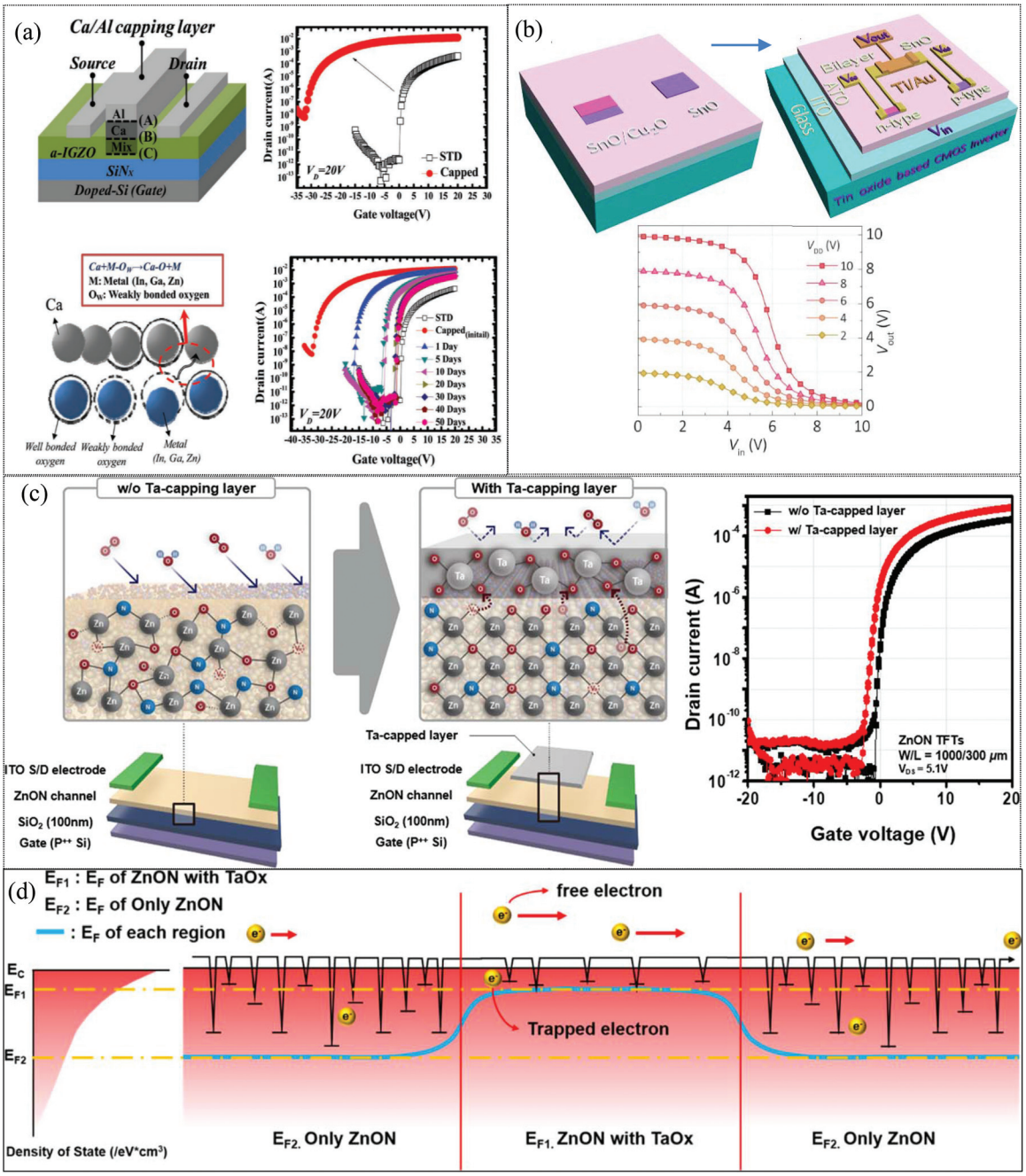

Fig. 6 (a) Bottom-gate top-contact a-IGZO TFT (STD device) is capped with a Ca/Al dual layer and transfer characteristics of STD and of Ca/Al-capped a-IGZO TFTs with a 50 days storage test in air (reproduced from ref. 132). (b) Schematic diagram of CMOS inverter fabrication and transfer curves of an optimized CMOS inverter (reproduced from ref. 133). (c) Schematic diagram of Ta-capped ZnON TFT P++ silicon wafer, transfer characteristics (d) schematic energy-band diagram dictated by trap-limited conduction (TLC) modulation for the Ta-capped ZnON TFTs (reproduced from ref. 135).

high electrostatic field (~50 MV mm^{-1}), ionic liquid (IL) gating has been extensively used to investigate electrostatic effects on fundamental physics problems in strongly correlated systems. These extremely high electric fields can extract or intercalate ionic species out of or into solids. Thus manipulation of the oxygen vacancy concentration *via* IL gating is a promising approach to tune the electrical properties, mitigating the need for high temperature annealing.[137,138] In 2019, Kulkarni *et al.* demonstrated athermal activation in an IWO channel TFT *via* an electrolyte-gating approach. Room temperature, RF sputtered IWO thin films (thickness ~7 nm) on SiO_2/Si wafers and on flexible substrates were activated by EMIM TFSI (1-ethyl-3-methylimidazolium bis(trifluoromethylsulfonyl)imide) ionic liquids. This technique facilitated the activation of non-func-

tioning TFTs to working transistors with a mobility of μ_{FE} = 7.1 cm^2 V^{-1} s^{-1} and $I_{ON/OFF}$ = 10^6 (back gate) and ionic-gated transistors with μ_{FE} = 105.4 cm^2 V^{-1} s^{-1} on flexible substrates at room temperature. Modulation of the local electronic structure of the channel by migrating oxygen species across the semiconductor–dielectric interface generated sufficient carriers for charge transport and for activation of oxygen-compensated thin films.[137] In 2016, Pudasaini *et al.* demonstrated IL gating of a-IGZO with a 1-hexyl-3-methylimidazolium bis (trifluoromethylsulfonyl) imide ([Hmim][TFSI]) ionic liquid to modulate the oxygen concentration in the channel layer and tune the threshold voltage (V_{th}). The ionic liquid was dispensed to cover the a-IGZO active area and auxiliary gate electrode as shown in Fig. 7b. The strong electric field induced by the electrical-double layer (EDL) formed at the interface between the IL and a-IGZO surface was responsible for the extraction of oxygen in the IGZO layer. A relatively large ON current (≈50 μA) with an $I_{ON/OFF}$ = 10^5 and μ_{FE} = 23.2 cm^2 V^{-1} s^{-1} was obtained for the athermal activated IL side gated a-IGZO TFT.[138] In 2013, J. Jeong *et al.* showed an electrolyte gating approach which suppresses the metal-to-insulator transition and stabilizes the metallic phase to temperatures below 5 kelvin for epitaxial thin films of VO_2, even after the ionic liquid is completely removed. These large electrostatic fields have been shown to be capable of moving ions in/out of other oxides as well (VO_2 and $SrTiO_3$).[139] In 2011, K. Ueno *et al.* demonstrated an unexpected superconducting phase in $KTaO_3$ by an ionic gating approach. EDL transistor devices were fabricated on $KTaO_3$ single crystals with an ionic liquid (as shown in Fig. 7a) with high I_{ON}/I_{OFF} >1 × 10^5. After biasing the ionic gate, electrostatic carrier doping could induce superconductivity in $KTaO_3$.[140] These novel oxygen vacancy modulation techniques facilitate low temperature activation of devices on flexible substrates. However, the modulation of oxygen vacancies is still debated as some researchers continue to suspect the changes to be related to movements of other ions (H^+ and OH^-) present in the ionic liquid.[141] For electronic gating on flexible substrates, having a liquid on top of the device may not be feasible; thus researchers are trying to form ionic gels which are mainly ABA type tri-block copolymers which consist of ionic liquid-phobic A blocks and ionic liquid-philic B blocks. Ionic liquids can absorb water and could also induce chemical reaction on prolonged exposure; hence care should be taken to minimize contact with water/humidity and other reactive elements.

2.2 Chemical routes for reduction of process temperature

For solution-processed metal oxide films deposited from precursor solutions, the as-deposited thin films consist of metal cation complexes, hydroxides, oxides *etc*. During the subsequent high temperature annealing, the M–O–M network is formed through a condensation process and complete anion

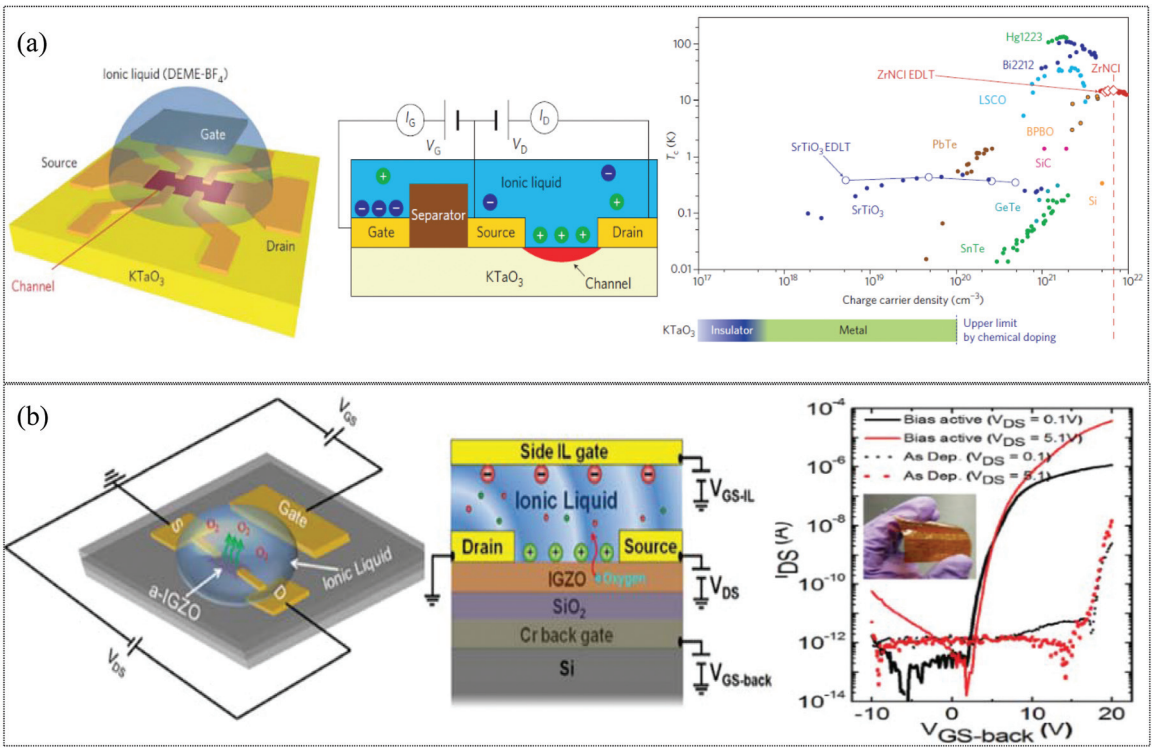

Fig. 7 (a) Electric double-layer (EDL) $KTaO_3$ transistor and superconducting critical temperature T_c as a function of three-dimensional charge carrier density for chemical doping induced superconductivity in 11 different materials systems (filled symbols), and electrostatically induced superconductivity in two of these (open symbols) (reproduced from ref. 140). (b) Dual-side gated a-IGZO TFT on a silicon substrate used for field induced activation testing and transfer characteristics of an IL gate activated flexible IGZO TFT (reproduced from ref. 138).

decomposition and organic residue removal. If insufficient thermal energy is available for the consumption of hydroxides and the decomposition of anions, the M–O–M structure formation and oxygen vacancy formation are affected and excess trap sites are generated, leading to degraded TFT device characteristics.

2.2.1 Precursor and solvent selection. For the precursor route of metal oxide film formation for MO thin film transistors, the choice of the precursor and solvent plays a vital role in the structural and electrical properties of the resultant metal oxide film. The figures of merit of a TFT such as the mobility, subthreshold swing and threshold voltage are predominantly influenced by the physical properties of the films such as M–O, M–OH and oxygen vacancy content, density, defect concentration, the presence of impurities *etc.* and these are in-turn dependent on the precursors and solvent utilized. Of the various metal precursors available, chlorides, acetates and nitrates have been widely adopted for the formation of metal oxide films.[142] A comprehensive study has been conducted by Kim *et al*. to investigate and analyze the effect of precursors and solvent on MO TFTs.[143] The mobility and threshold voltage of the fabricated MO TFTs are influenced by the type of precursor and type of solvent, respectively, (Fig. 8a). Analytical studies proved that the precursor type affected the trap density and also the band mobility, which is an indication of s orbital overlap, while the solvent, which determines the metal-ion complex formed in the precursor solution, affected the deep level traps, dependent on the number of metal interstitials. Of the various precursors, nitrate-based MO-films demonstrated the highest field-effect mobility and lowest trap density, while the use of acetonitrile as the solvent leads to the highest threshold voltage. XPS investigations corroborated the findings and illustrated that the nitrate-based films display the lowest M–OH content, resulting in reduced trap density and the largest M–O to M–OH bond area ratio, resulting in the highest s orbital overlap. The precursor type was also found to affect the density of the film formed and hence the mobility, by virtue of the volume of the decomposed ions and atoms in the precursors. Nitrates also yielded MO films with the highest density while chlorides by virtue of their inherent defects yielded MO films with the lowest density. Among the various metal precursors used such as chlorides, acetates and nitrates, the latter also shows the weakest anion complexation, which ensures complete anion decomposition at lower temperatures.[144] The use of nitrate precursors thus provides an approach to reduce the thermal energy required for the formation of high-quality MO films with reduced hydrates and other M–O–M network disrupting impurities by virtue of anions capable of lower temperature decomposition, as is evident from the thermogravimetric studies (Fig. 8b). Metal alkoxides are a class of precursors, which afford the formation of metal oxide films at low temperatures in the presence of an aqueous catalyst or in an aqueous environment. H. Sirringhaus *et al.* have demonstrated a sol–gel on chip process using an indium alkoxide cluster and zinc-bis-methoxyethoxide in which an *in situ* process involved the use of a controlled amount of water vapor to facilitate hydrolysis on the surface of a spin coated film, resulting in metal–oxide film formation at a low temperature of 230 °C with a low M–OH content. The fabricated TFT exhibited a mobility of 10 $cm^2\ V^{-1}\ s^{-1}$, V_{on} = 0 V, high I_{on}/I_{off}[108] and low hysteresis with stable, repeatable performance and high operational stability.[145] Solution processed MO TFTs typically employ 2-methoxy ethanol or similar alcohol-based solvents for precursor solutions. Recently, water has emerged as a contender by virtue of its ability to form carbon residue-free films at low processing temperature.[66,146,147] Ionic species dissociation is promoted by the high polarity and high dielectric constant (~80) of the aqueous solvent and by acting as a sigma donor, resulting in the formation of hexaaqua complexes as shown in Fig. 8d. Water, when used for the fabrication of both Al_2O_3 dielectric and In_2O_3 films, resulted in TFTs with a mobility of ~38 $cm^2\ V^{-1}\ s^{-1}$ and an I_{on}/I_{off} of 10^7 at a processing temperature of 250 °C.[148] The duration and temperature at which aqueous precursors are processed before spin-coating also exhibit significant impact on the MO film formed. According to Park *et al.*, precursors retained at 70 °C for longer durations (12–72 h) have a higher concentration of dissociated cations which results in a higher concentration of hexaaqua metal ion complexes, critical for the low temperature metal oxide formation using the aqueous route.[59]

2.2.2 Combustion synthesis. As discussed, in the case of solution-processed metal oxides, low temperature annealing results in incomplete metal oxide formation and hydroxyl group rich films. A universal and facile method to reduce the processing temperature of solution-processed metal oxide films *viz.*, combustion synthesis, was demonstrated by Kim *et al.*, in 2011.[149] In the combustion synthesis approach, a fuel additive triggers a localized exothermic reaction with metal nitrate precursors (oxidisers), thereby providing sufficient energy to eliminate the need for a subsequent high temperature annealing for M–O–M network formation and residue removal (Fig. 8e). Acetyl acetone and urea are the commonly used fuels for combustion synthesis of metal oxide films.[150–153] Facchetti *et al.* reported that the addition of an oxidizing NO_2 group to an acetylacetone fuel results in an enthalpy of combustion of 988.6 compared to 784.4 J g^{-1} of acetyl acetone and an ignition temperature of 107.8 °C compared to 166.5 °C of acetylacetone (Fig. 8f).[154] This results in a lowering of the processing temperature for the formation of metal oxide films while simultaneously resulting in denser films with a higher M–O–M content. Non-toxic and environmentally safe carbohydrates such as sorbitol, sucrose and glucose as co-fuels have been shown to be effective at increasing the enthalpy of the overall reaction.[155] Their optimized incorporation into the fuel system results in a dense, smooth, high-quality metal oxide content as is clear from XPS and thickness measurements, where the M–O–M to total O 1s peak ratio and film densification are the highest at a 10% sugar content, as shown in Fig. 8g, with the higher sugar content adversely affecting the film formation due to exploitation of oxidizers for excess sugar decomposition and the generation of

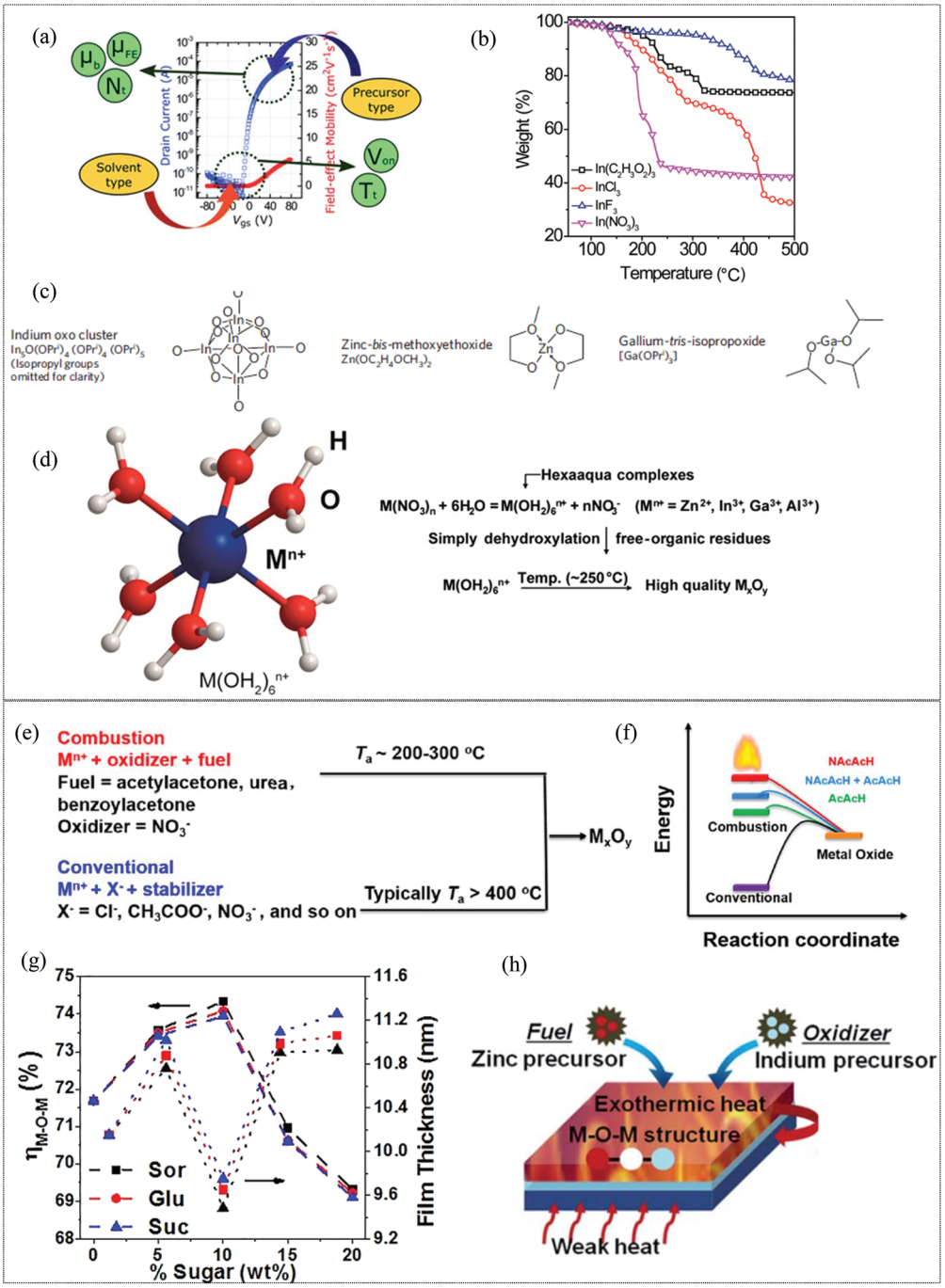

Fig. 8 (a) Illustration of the effect of the solvent and precursor type on the TFT device characteristics (reproduced from ref. 143), (b) thermogravimetric analyses of the various aqueous metal precursors of $In(C_2H_3O_2)_3$, $InCl_3$, InF_3, and $In(NO_3)_3$ (reproduced from ref. 148), (c) various alkoxide derivatives used for metal oxide formation (reproduced from ref. 145), (d) structure of the hexaaqua complexes formed in aqueous solvent and the progress of reactions resulting in the formation of metal oxide films (reproduced from ref. 148), (e) combustion *vs.* conventional synthetic approaches (reproduced from ref. 149), (f) energetics of combustion synthesis for various fuels (reproduced from ref. 154), (g) XPS O 1s M–O–M peak area to total peak area ratio and film thickness *vs.* sugar concentration (reproduced from ref. 155), and (h) schematic diagram of combustion synthesis *via* the use of metal precursors bearing the fuel and oxidizer ligands (reproduced from ref. 156).

impurities. With a prudent choice of metal precursors which can act as the source of both the oxidizer and fuel (Fig. 8h), Cho *et al.* have demonstrated that a self-combustion synthesis can also be activated in a two-component precursor system without the need for further fuels or additives.[156] Combustion synthesis is a viable method for reducing the processing temperature as it is independent of any additional post-processing steps and is readily scalable. However, though combustion can

proceed at temperatures as low as 100 °C, a higher temperature of around 200–300 °C is required to ensure adequate decomposition of the precursors to ignite the combustion, especially since nitrates are generally oxidizers for the combustion synthesis. Due to the thermal ignition required, combustion synthesis is often used in conjunction with CTA, thus requiring a long duration for activation. In addition, the oxygen vacancy generation during the combustion synthesis is determined by the reaction environment, oxygen generated during the combustion reaction and post-treatment. For high performance metal oxide films, a precise control of the reaction environment during processing is thus imperative.[157]

3. Other low temperature processing approaches

Plasma treatment using hydrogen, argon *etc.* has also been used for sputtered MO films to improve the device performance under low temperature processing conditions and has also been extended to solution processed MO TFTs.[158,159] Plasma treatment using hydrogen has been used for the decomposition of residual organic species subsequent to the formation of metal oxide layers. This treatment followed by an oxidation step has been shown to increase the stability of the device while improving the TFT device performance.[160] There have recently been reports on the use of NH_3 and N_2O plasma treatments resulting in improved device performance.[161,162] Other novel techniques include water vapour annealing,[163] where the presence of water vapor leads to efficient hydrolysis reaction for solution processed MO films, resulting in higher M–O and lower M–OH concentrations and photocatalytic reactions using TiO_2 under UV irradiation for decomposition of organic residues and defect site reduction.[164] In addition to these novel methods, a combination of various annealing conditions and techniques has been shown to result in improved performance of MO TFTs. Combining plasma treatment with (a) thermal annealing,[165] (b) atmospheric pressure treatment[166] or (c) microwave irradiation[167] has been shown to drastically improve TFT performance.

4. Conclusions and outlook

Significant research effort is being dedicated to achieving low temperature processing for MO TFTs, thus enabling their widespread application in flexible electronics. Conventional annealing techniques such as high-temperature thermal annealing, rapid thermal annealing, laser annealing *etc.* require high temperature to tune the oxygen vacancy in the metal oxide semiconductor which results in adverse effects on flexible substrates. Replacing the high thermal budget required for such conventional annealing with photochemical, plasma-assisted and microwave annealing techniques is applicable to both vacuum deposited and solution processed MO TFTs. In the case of solution processed MO films, additional avenues are available such as appropriate selection of precursors, solvents and fuel additives for aiding in combustion synthesis, and reducing the process temperature for the formation of high-quality metal oxide films. However, all these techniques except for laser annealing are nonselective, *i.e.*, all the TFTs on the substrates are affected by the process. If selective annealing is required, a complex number of steps will be required, such as photolithography, to tune the attributes of the thin film semiconductor selectively. As discussed in this review, another promising alternative is the athermal oxygen vacancy modulation and defect passivation of the metal oxide film for tailoring the electronic structure, which makes high temperature treatments, typically critical for achieving high performance TFTs, dispensable. Athermal activation using a capping layer or an ionic liquid paves the way for flexible and transparent electronics. In the ionic liquid gating approach, which is limited to charge modulation and accumulation for an ionic liquid TFT, the high electric field of the order of 50 MV mm^{-1} present at the interface due to Helmholtz layers can be used to vary the oxygen ions present in the film. The controlled manipulation of oxygen vacancies changes the conductance of the film in a precise manner which is of interest for novel applications such as neuromorphic electronics. Such techniques also allow for selective treatments on individual TFTs within a large substrate. The metal capping layer approach facilitates the decrease of weakly bonded oxygen density or reduction in the defect density by partial crystallization of the underlying AOS layer at low temperature. This structure has shown high μ_{FE} and enhanced stability simply by adopting a selective metal capping layer while ensuring reduction in the process temperature as discussed in the above sections. Apart from the options discussed in the review, manipulation of the active layer structure is another viable alternative for achieving high performance metal oxide TFTs. Hybrid metal oxide-2D TFTs have been investigated, where the addition of high conductivity 2D materials, such as graphene/CNT, in the active layer stack leads to enhanced TFT mobility. Hybrid metal oxide-2D heterostructure and quasi-superlattice metal oxide stacks are another class of active layers employed for realizing high mobility TFTs at low processing temperature. According to reports, the ultrathin metal oxide layers that form these active layers enable the manifestation of a 2D charge transport phenomenon, while the incorporation of a deep Fermi level metal oxide in the stack results in a higher I_{on}/I_{off} ratio. Compared to initial research studies, effort is now being made to ensure that the methods used for enhanced device performance at lower processing temperatures do not adversely affect the device stability. Metal oxide semiconductors are also highly sensitive to their atmosphere, and exposure to moisture and oxygen can affect device stability, an issue which needs to be addressed. As discussed, researchers have reported that using capping layers, such as Al_2O_3, SiO_2, Y_2O_3, HfO_2, ZrO_2, TiO_2, AHO (Al_2O_3-HfO_2 stack) and ATO (Al_2O_3, TiO_2 stack) can improve the stability of oxide semiconductors in air and at higher temperatures. In addition, the scalability and production-line compatibility of the various techniques for redu-

cing the processing temperature of metal oxide semiconductors should also be thoroughly examined. With continued research efforts being made to realize stability, scalability and low temperature processing, metal oxide thin films are the most promising material system for propelling flexible and transparent electronics into a ubiquitous technology.

Conflicts of interest

There are no conflicts to declare.

Acknowledgements

The authors would like to acknowledge the funding from the MOE Tier 1 Grant RG 166/16 and the MOE Tier 2 Grant MOE2016-T2-1-100.

Notes and references

1 J. K. Jeong, Photo-bias instability of metal oxide thin film transistors for advanced active matrix displays, *J. Mater. Res.*, 2013, **28**(16), 2071–2084.
2 N. Tiwari, H. P. D. Shieh and P. T. Liu, Structural, optical, and photoluminescence study of ZnO/IGZO thin film for thin film transistor application, *Mater. Lett.*, 2015, **151**, 53–56.
3 W. Xu, H. Li, J. B. Xu and L. Wang, Recent Advances of Solution-Processed Metal Oxide Thin-Film Transistors, *ACS Appl. Mater. Interfaces*, 2018, **10**(31), 25878–25901.
4 N. Tiwari, R. N. Chauhan, H. P. D. Shieh, P. T. Liu and Y. P. Huang, Photoluminescence and Reliability Study of ZnO Cosputtered IGZO Thin-Film Transistors under Various Ambient Conditions, *IEEE Trans. Electron Devices*, 2016, **63**(4), 1578–1581.
5 N. Tiwari, R. N. Chauhan, P. T. Liu and H. P. D. Shieh, Electrical characteristics of InGaZnO thin film transistor prepared by co-sputtering dual InGaZnO and ZnO targets, *RSC Adv.*, 2015, **5**(64), 51983–51989, DOI: 10.1039/C5RA08793G.
6 R. Chen and L. Lan, Solution-processed metal-oxide thin-film transistors: a review of recent developments, *Nanotechnology*, 2019, **30**(31), 312001, DOI: 10.1088/1361-6528/ab1860.
7 E. Fortunato, P. Barquinha and R. Martins, Oxide semiconductor thin-film transistors: A review of recent advances, *Adv. Mater.*, 2012, **24**(22), 2945–2986.
8 L. Petti, N. Münzenrieder, C. Vogt, H. Faber, L. Büthe, G. Cantarella, *et al.*, Metal oxide semiconductor thin-film transistors for flexible electronics, *Appl. Phys. Rev.*, 2016, **3**(2), 021303-53.
9 Y. H. Zhang, Z. X. Mei, H. L. Liang and X. L. Du, Review of flexible and transparent thin-film transistors based on zinc oxide and related materials, *Chin. Phys. B*, 2017, **26**(4), 047307-17.
10 H. Hosono, Ionic amorphous oxide semiconductors: Material design, carrier transport, and device application, *J. Non-Cryst. Solids*, 2006, **352**(9-20 SPEC. ISS.), 851–858.
11 J. Sheng, H. J. Jeong, K. L. Han, T. H. Hong and J. S. Park, Review of recent advances in flexible oxide semiconductor thin-film transistors, *J. Inf. Disp.*, 2017, **18**(4), 159–172, DOI: 10.1080/15980316.2017.1385544.
12 R. Chen and L. Lan, Transistors: a Review of Recent Developments, *Nanotechnology*, 2019, **30**(31), 312001.
13 J. F. Wager, B. Yeh, R. L. Hoffman and D. A. Keszler, An amorphous oxide semiconductor thin-film transistor route to oxide electronics, *Curr. Opin. Solid State Mater. Sci.*, 2014, **18**(2), 53–61, DOI: 10.1016/j.cossms.2013.07.002.
14 J. Yeon Kwon and J. Kyeong Jeong, Recent progress in high performance and reliable n-type transition metal oxide-based thin film transistors, *Semicond. Sci. Technol.*, 2015, **30**(2), 024002.
15 J. S. Seo, J. H. Jeon, Y. H. Hwang, H. Park, M. Ryu, S. H. K. Park, *et al.*, Solution-processed flexible fluorine-doped indium zinc oxide thin-film transistors fabricated on plastic film at low temperature, *Sci. Rep.*, 2013, **3**, 1–9.
16 S. Parthiban and J. Y. Kwon, Role of dopants as a carrier suppressor and strong oxygen binder in amorphous indium-oxide-based field effect transistor, *J. Mater. Res.*, 2014, **29**(15), 1585–1596.
17 H. D. Kim, J. H. Kim, K. Park, Y. C. Park, S. Kim, Y. J. Kim, *et al.*, Highly Stable Thin-Film Transistors Based on Indium Oxynitride Semiconductor, *ACS Appl. Mater. Interfaces*, 2018, **10**(18), 15873–15879.
18 https://www.adnano-tek.com.
19 S. Jeong and J. Moon, Low-temperature, solution-processed metal oxide thin film transistors, *J. Mater. Chem.*, 2012, **22**(4), 1243–1250, DOI: 10.1039/C1JM14452A.
20 J. W. Jo, Y. H. Kim and S. K. Park, Light-induced hysteresis and recovery behaviors in photochemically activated solution-processed metal-oxide thin-film transistors, *Appl. Phys. Lett.*, 2014, **105**(4), 043503.
21 B. D. Ahn, H. J. Jeon, J. Sheng, J. Park and J. S. Park, A review on the recent developments of solution processes for oxide thin film transistors, *Semicond. Sci. Technol.*, 2015, **30**(6), 064001.
22 Dhananjay and C. W. Chu, Realization of In2 O3 thin film transistors through reactive evaporation process, *Appl. Phys. Lett.*, 2007, **91**(13), 2005–2008.
23 J. C. Park, C. J. Kim and S. Im, High performance self-aligned top-gate amorphous indium zinc oxide thin-film transistors, *Proc 20th Int Work Act Flatpanel Displays Devices TFT Technol FPD Mater AM-FPD 2013*, 2013, pp. 247–50.
24 T. Kizu, S. Aikawa, N. Mitoma, M. Shimizu, X. Gao, M. F. Lin, *et al.*, Low-temperature processable amorphous In-W-O thin-film transistors with high mobility and stability, *Appl. Phys. Lett.*, 2014, **104**(15), 1–6.
25 P. T. Liu, C. H. Chang and C. J. Chang, Reliability enhancement of high-mobility amorphous indium-tung-

sten oxide thin film transistor, *ECS Trans.*, 2015, **67**(1), 9–16.

26 M. Qu, C. H. Chang, T. Meng, Q. Zhang, P. T. Liu and H. P. D. Shieh, Stability study of indium tungsten oxide thin-film transistors annealed under various ambient conditions, *Phys. Status Solidi A*, 2017, **214**(2), 2–5.

27 D. Lin, S. Pi, J. Yang, N. Tiwari, J. Ren, Q. Zhang, *et al.*, Enhanced stability of thin film transistors with double-stacked amorphous IWO/IWO:N channel layer, *Semicond. Sci. Technol.*, 2018, **33**(6), 065001.

28 R. N. Chauhan, N. Tiwari, H. P. D. Shieh and P. T. Liu, Electrical performance and stability of tungsten indium zinc oxide thin-film transistors, *Mater. Lett.*, 2018, **214**, 293–296, DOI: 10.1016/j.matlet.2017.12.020.

29 J. Sheng, T. Hong, D. Kang, Y. Yi, J. H. Lim and J. S. Park, Design of InZnSnO Semiconductor Alloys Synthesized by Supercycle Atomic Layer Deposition and Their Rollable Applications, *ACS Appl. Mater. Interfaces*, 2019, **11**(13), 12683–12692.

30 M. H. Cho, H. Seol, H. Yang, P. S. Yun, J. U. Bae, K. S. Park, *et al.*, High-Performance Amorphous Indium Gallium Zinc Oxide Thin-Film Transistors Fabricated by Atomic Layer Deposition, *IEEE Electron Device Lett.*, 2018, **39**(5), 688–691.

31 Y. J. Tak, F. Hilt, S. Keene, W. G. Kim, R. H. Dauskardt, A. Salleo, *et al.*, High-Throughput Open-Air Plasma Activation of Metal-Oxide Thin Films with Low Thermal Budget, *ACS Appl. Mater. Interfaces*, 2018, **10**(43), 37223–37232.

32 J. W. Park, Y. J. Tak, J. W. Na, H. Lee, W. G. Kim and H. J. Kim, Effect of Static and Rotating Magnetic Fields on Low-Temperature Fabrication of InGaZnO Thin-Film Transistors, *ACS Appl. Mater. Interfaces*, 2018, **10**(19), 16613–16622.

33 K. S. Kim, C. H. Ahn, S. H. Jung, S. W. Cho and H. K. Cho, Toward Adequate Operation of Amorphous Oxide Thin-Film Transistors for Low-Concentration Gas Detection, *ACS Appl. Mater. Interfaces*, 2018, **10**(12), 10185–10193, DOI: 10.1021/acsami.7b18657.

34 J. H. Park, Y. G. Kim, S. Yoon, S. Hong and H. J. Kim, Simple method to enhance positive bias stress stability of In-Ga-Zn-O thin-film transistors using a vertically graded oxygen-vacancy active layer, *ACS Appl. Mater. Interfaces*, 2014, **6**(23), 21363–21368.

35 W. Xu, M. Xu, J. Jiang, C. Luan, L. Han and X. Feng, High Performance Thin Film Transistors with Sputtered In-Al-Zn-O Channel and Different Source/Drain Electrodes, *IEEE Electron Device Lett.*, 2019, **40**(2), 247–250.

36 T. H. Cheng, S. P. Chang and S. J. Chang, Electrical Properties of Indium Aluminum Zinc Oxide Thin Film Transistors, *J. Electron. Mater.*, 2018, **47**(11), 6923–6928.

37 Y. Cong, D. Han, J. Dong, S. Zhang, X. Zhang and Y. Wang, Fully transparent high performance thin film transistors with bilayer ITO/Al-Sn-Zn-O channel structures fabricated on glass substrate, *Sci. Rep.*, 2017, **7**(1), 1–6, DOI: 10.1038/s41598-017-01691-7.

38 H. J. Jeong, H. M. Lee, C. H. Ryu, E. J. Park, K. L. Han, H. J. Hwang, *et al.*, Ultra-High-Speed Intense Pulsed-Light Irradiation Technique for High-Performance Zinc Oxynitride Thin-Film Transistors, *ACS Appl. Mater. Interfaces*, 2019, **11**(4), 4152–4158.

39 C. W. Shih, T. J. Yen, A. Chin, C. F. Lu and W. F. Su, Low-Temperature Processed Tin Oxide Transistor with Ultraviolet Irradiation, *IEEE Electron Device Lett.*, 2019, **40**(6), 909–912.

40 J. Lee, J. Moon, J. E. Pi, S. D. Ahn, H. Oh, S. Y. Kang, *et al.*, High mobility ultra-thin crystalline indium oxide thin film transistor using atomic layer deposition, *Appl. Phys. Lett.*, 2018, **113**(11), 112102-5.

41 Q. Ma, H. M. Zheng, Y. Shao, B. Zhu, W. J. Liu, S. J. Ding, *et al.*, Atomic-Layer-Deposition of Indium Oxide Nano-films for Thin-Film Transistors, *Nanoscale Res. Lett.*, 2018, **13**(1), 2–9.

42 C. H. Ahn, K. Senthil, H. K. Cho and S. Y. Lee, Artificial semiconductor/insulator superlattice channel structure for high-performance oxide thin-film transistors, *Sci. Rep.*, 2013, **3**, 1–6.

43 H. Xu, M. Xu, Z. Chen, M. Li, J. Zou, H. Tao, *et al.*, Improvement of Mobility and Stability in Oxide Thin-Film Transistors Using Triple-Stacked Structure, *IEEE Electron Device Lett.*, 2016, **37**(1), 57–59.

44 H. S. Kim, J. S. Park, H. K. Jeong, K. S. Son, T. S. Kim, J. B. Seon, *et al.*, Density of states-based design of metal oxide thin-film transistors for high mobility and superior photostability, *ACS Appl. Mater. Interfaces*, 2012, **4**(10), 5416–5421.

45 H. Xu, M. Xu, M. Li, Z. Chen, J. Zou, W. Wu, *et al.*, Trap-Assisted Enhanced Bias Illumination Stability of Oxide Thin Film Transistor by Praseodymium Doping, *ACS Appl. Mater. Interfaces*, 2019, **11**(5), 5232–5239.

46 R. N. Chauhan, N. Tiwari, P. T. Liu, H. P. D. Shieh and J. Kumar, Silicon induced stability and mobility of indium zinc oxide based bilayer thin film transistors, *Appl. Phys. Lett.*, 2016, **109**(20), 202107-5.

47 N. Tiwari, R. N. Chauhan, P. T. Liu and H. P. D. Shieh, Modification of intrinsic defects in IZO/IGZO thin films for reliable bilayer thin film transistors, *RSC Adv.*, 2016, **6**(79), 75393–75398.

48 Y. Le, Y. Shao, X. Xiao, X. Xu and S. Zhang, Indium-Tin-Oxide Thin-Film Transistors With In Situ Anodized Ta2O5 Passivation Layer, *IEEE Electron Device Lett.*, 2016, **37**(5), 603–606.

49 X. Xu, L. Zhang, Y. Shao, Z. Chen, Y. Le and S. Zhang, Amorphous Indium Tin Oxide Thin-Film Transistors Fabricated by Cosputtering Technique, *IEEE Trans. Electron Devices*, 2016, **63**(3), 1072–1077.

50 J. Sheng, E. J. Park, B. Shong and J. S. Park, Atomic Layer Deposition of an Indium Gallium Oxide Thin Film for Thin-Film Transistor Applications, *ACS Appl. Mater. Interfaces*, 2017, **9**(28), 23934–23940.

51 W.-L. Huang, M.-H. Hsu, S.-P. Chang, S.-J. Chang and Y.-Z. Chiou, Indium Gallium Oxide Thin Film Transistor

for Two-Stage UV Sensor Application, *ECS J. Solid State Sci. Technol.*, 2019, **8**(7), Q3140–Q3143.
52 Y. H. Lin and J. C. Chou, Temperature effects on a-IGZO thin film transistors using HfO2 gate dielectric material, *J. Nanomater.*, 2014, **2014**, 2–7.
53 C. Liu, Y. Sun, H. Qin, Y. Liu, S. Wei and Y. Zhao, Low-Temperature, High-Performance InGaZnO Thin-Film Transistors Fabricated by Capacitive Coupled Plasma-Assistant Magnetron Sputtering, *IEEE Electron Device Lett.*, 2019, **40**(3), 415–418.
54 P. Ma, L. Du, Y. Wang, R. Jiang, Q. Xin, Y. Li, *et al.*, Low voltage operation of IGZO thin film transistors enabled by ultrathin Al2O3 gate dielectric, *Appl. Phys. Lett.*, 2018, **112**(2), 1–5.
55 W. Cai, S. Park, J. Zhang, J. Wilson, Y. Li, Q. Xin, *et al.*, One-Volt IGZO Thin-Film Transistors with Ultra-Thin, Solution-Processed Al x O y Gate Dielectric, *IEEE Electron Device Lett.*, 2018, **39**(3), 375–378.
56 J. S. Hur, J. O. Kim, H. A. Kim and J. K. Jeong, Stretchable Polymer Gate Dielectric by Ultraviolet-Assisted Hafnium Oxide Doping at Low Temperature for High-Performance Indium Gallium Tin Oxide Transistors, *ACS Appl. Mater. Interfaces*, 2019, **11**(24), 21675–21685.
57 H. S. Kim and J. S. Park, The performance and negative bias illumination stability of Hf-In-Zn-O thin film transistors on sputtering conditions, *J. Electroceram.*, 2014, **32**(2–3), 220–223.
58 B. Wang, P. Guo, L. Zeng, X. Yu, A. Sil, W. Huang, *et al.*, Expeditious, scalable solution growth of metal oxide films by combustion blade coating for flexible electronics, *Proc. Natl. Acad. Sci. U. S. A.*, 2019, **116**(19), 9230–9238.
59 J. Park, T. Gergely, Y. S. Rim and S. Pyo, Significant Performance Improvement of Solution-Processed Metal Oxide Transistors by Ligand Dissociation through Coupled Temperature–Time Treatment of Aqueous Precursors, *ACS Appl. Electron. Mater.*, 2019, **1**(4), 505–512, DOI: 10.1021/acsaelm.8b00117.
60 Y. Li, W. Xu, W. Liu, S. Han, P. Cao, M. Fang, *et al.*, High-Performance Thin-Film Transistors with Aqueous Solution-Processed NiInO Channel Layer, *ACS Appl. Electron. Mater.*, 2019, **1**(9), 1842–1851.
61 X. Chen, G. Zhang, J. Wan, T. Guo, L. Li, Y. Yang, *et al.*, Transparent and Flexible Thin-Film Transistors with High Performance Prepared at Ultralow Temperatures by Atomic Layer Deposition, *Adv. Electron. Mater.*, 2019, **5**(2), 1–8.
62 H. U. Li and T. N. Jackson, Oxide semiconductor thin film transistors on thin solution-cast flexible substrates, *IEEE Electron Device Lett.*, 2015, **36**(1), 35–37.
63 Y. Zhang, Z. Mei, S. Cui, H. Liang, Y. Liu and X. Du, Flexible Transparent Field-Effect Diodes Fabricated at Low-Temperature with All-Oxide Materials, *Adv. Electron. Mater.*, 2016, **2**(5), 1–5.
64 L. W. Ji, C. Z. Wu, T. H. Fang, Y. J. Hsiao, T. H. Meen, W. Water, *et al.*, Characteristics of flexible thin-film transistors with zno channels, *IEEE Sens. J*, 2013, **13**(12), 4940–4943.
65 C. Y. Lee, M. Y. Lin, W. H. Wu, J. Y. Wang, Y. Chou, W. F. Su, *et al.*, Flexible ZnO transparent thin-film transistors by a solution-based process at various solution concentrations, *Semicond. Sci. Technol.*, 2010, **25**(10), 105008.
66 Y. Lin, H. Faber, K. Zhao, Q. Wang, A. Amassian, M. Mclachlan, *et al.*, High-Performance ZnO Transistors Processed Via an Aqueous Carbon-Free Metal Oxide Precursor Route at Temperatures Between 80–180° C, *Adv. Mater.*, 2013, 4340–4346.
67 D. Zhao, D. A. Mourey and T. N. Jackson, Fast flexible plastic substrate ZnO circuits, *IEEE Electron Device Lett.*, 2010, **31**(4), 323–325.
68 K. Hong, S. H. Kim, K. H. Lee and C. D. Frisbie, Printed, sub-2V ZnO electrolyte gated transistors and inverters on plastic, *Adv. Mater.*, 2013, **25**(25), 3413–3418.
69 Y. S. Li, J. C. He, S. M. Hsu, C. C. Lee, D. Y. Su, F. Y. Tsai, *et al.*, Flexible Complementary Oxide-Semiconductor-Based Circuits Employing n-Channel ZnO and p-Channel SnO Thin-Film Transistors, *IEEE Electron Device Lett.*, 2016, **37**(1), 46–49.
70 S. Park, K. Cho, K. Yang and S. Kim, Electrical characteristics of flexible ZnO thin-film transistors annealed by microwave irradiation, *J. Vac. Sci. Technol., B: Nanotechnol. Microelectron.: Mater., Process., Meas., Phenom.*, 2014, **32**(6), 062203, DOI: 10.1116/1.4898115.
71 K. Park, D. K. Lee, B. S. Kim, H. Jeon, N. E. Lee, D. Whang, *et al.*, Stretchable, transparent zinc oxide thin film transistors, *Adv. Funct. Mater.*, 2010, **20**(20), 3577–3582.
72 K. Song, J. Noh, T. Jun, Y. Jung, H. Y. Kang and J. Moon, Fully flexible solution-deposited ZnO thin-film transistors, *Adv. Mater.*, 2010, **22**(38), 4308–4312.
73 Y. Jung, T. Jun, A. Kim, K. Song, T. H. Yeo and J. Moon, Direct photopatternable organic-inorganic hybrid gate dielectric for solution-processed flexible ZnO thin film transistors, *J. Mater. Chem.*, 2011, **21**(32), 11879–11885.
74 S. H. Kim, J. Yoon, S. O. Yun, Y. Hwang, H. S. Jang and H. C. Ko, Ultrathin sticker-type ZnO thin film transistors formed by transfer printing via topological confinement of water-soluble sacrificial polymer in dimple structure, *Adv. Funct. Mater.*, 2013, **23**(11), 1475–1482.
75 F. Fleischhaker, V. Wloka and I. Hennig, ZnO based field-effect transistors (FETs): Solution-processable at low temperatures on flexible substrates, *J. Mater. Chem.*, 2010, **20**(32), 6622–6625.
76 A. Zeumault, S. Ma and J. Holbery, Fully inkjet-printed metal-oxide thin-film transistors on plastic, *Phys. Status Solidi A*, 2016, **213**(8), 2189–2195.
77 J. Zhou, G. Wu, L. Guo, L. Zhu and Q. Wan, Flexible transparent junctionless TFTs with oxygen-tuned indium-zinc-oxide channels, *IEEE Electron Device Lett.*, 2013, **34**(7), 888–890.
78 W. Yang, K. Song, Y. Jung, S. Jeong and J. Moon, Solution-deposited Zr-doped AlO x gate dielectrics enabling high-performance flexible transparent thin film transistors, *J. Mater. Chem. C*, 2013, **1**(27), 4275–4282.

79 L. R. Zhang, C. Y. Huang, G. M. Li, L. Zhou, W. J. Wu, M. Xu, *et al.*, A Low-Power High-Stability Flexible Scan Driver Integrated by IZO TFTs, *IEEE Trans. Electron Devices*, 2016, **63**(4), 1779–1782.

80 B. Wang, X. Yu, P. Guo, W. Huang, L. Zeng, N. Zhou, *et al.*, Solution-Processed All-Oxide Transparent High-Performance Transistors Fabricated by Spray-Combustion Synthesis, *Adv. Electron. Mater.*, 2016, **2**(4), 1500427.

81 D. Wee, S. Yoo, Y. H. Kang, Y. H. Kim, J. W. Ka, S. Y. Cho, *et al.*, Poly(imide-benzoxazole) gate insulators with high thermal resistance for solution-processed flexible indium-zinc oxide thin-film transistors, *J. Mater. Chem. C*, 2014, **2**(31), 6395–6401.

82 N. Tiwari, M. Rajput, R. A. John, M. R. Kulkarni, A. C. Nguyen and N. Mathews, Indium Tungsten Oxide Thin Films for Flexible High-Performance Transistors and Neuromorphic Electronics, *ACS Appl. Mater. Interfaces*, 2018, **10**(36), 30506–30513.

83 J. Liu, D. B. Buchholz, R. P. H. Chang, A. Facchetti and T. J. Marks, High-performance flexible transparent thin-film transistors using a hybrid gate dielectric and an amorphous zinc indium tin oxide channel, *Adv. Mater.*, 2010, **22**(21), 2333–2337.

84 M. Nakata, G. Motomura, Y. Nakajima, T. Takei, H. Tsuji, H. Fukagawa, *et al.*, Development of flexible displays using back-channel-etched In-Sn-Zn-O thin-film transistors and air-stable inverted organic light-emitting diodes, *J. Soc. Inf. Disp.*, 2016, **24**(1), 3–11.

85 W. S. Cheong, J. Y. Bak and H. S. Kim, Transparent flexible zinc-indium-tin oxide thin-film transistors fabricated on polyarylate films, *Jpn. J. Appl. Phys.*, 2010, **49**(5 PART 2), 05EB10-4.

86 Y. S. Rim, H. Chen, Y. Liu, S. H. Bae, H. J. Kim and Y. Yang, Direct light pattern integration of low-temperature solution-processed all-oxide flexible electronics, *ACS Nano*, 2014, **8**(9), 9680–9686.

87 H. H. Hsu, C. Y. Chang and C. H. Cheng, A flexible IGZO thin-film transistor with stacked TiO2-based dielectrics fabricated at room temperature, *IEEE Electron Device Lett.*, 2013, **34**(6), 768–770.

88 N. C. Su, S. J. Wang, C. C. Huang, Y. H. Chen, H. Y. Huang, C. K. Chiang, *et al.*, Low-voltage-driven flexible InGaZnO thin-film transistor with small subthreshold swing, *IEEE Electron Device Lett.*, 2010, **31**(7), 680–682.

89 S.-W. Jung, *et al.*, Flexible nonvolatile memory transistors using indium gallium zinc oxide-channel and ferroelectric polymer poly (vinylidene fluoride-co-trifluoroethylene) fabricated on elastomer substrate, *J. Vac. Sci. Technol., B*, 2015, **33**(5), 51201.

90 M. Mativenga, M. H. Choi, J. W. Choi and J. Jang, Transparent flexible circuits based on amorphous-indium-gallium-zincoxide thin-film transistors, *IEEE Electron Device Lett.*, 2011, **32**(2), 170–172.

91 D. Karnaushenko, N. Münzenrieder, D. D. Karnaushenko, B. Koch, A. K. Meyer, S. Baunack, *et al.*, Biomimetic Microelectronics for Regenerative Neuronal Cuff Implants, *Adv. Mater.*, 2015, **27**(43), 6797–6805.

92 M. J. Park, D. J. Yun, M. K. Ryu, J. H. Yang, J. E. Pi, O. S. Kwon, *et al.*, Improvements in the bending performance and bias stability of flexible InGaZnO thin film transistors and optimum barrier structures for plastic poly (ethylene naphthalate) substrates, *J. Mater. Chem. C*, 2015, **3**(18), 4779–4786.

93 A. K. Tripathi, K. Myny, B. Hou, K. Wezenberg and G. H. Gelinck, Electrical Characterization of Flexible InGaZnO Transistors and 8-b Transponder Chip Down to a Bending Radius of 2 mm, *IEEE Trans. Electron Devices*, 2015, **62**(12), 4063–4068.

94 H. Xu, D. Luo, M. Li, M. Xu, J. Zou, H. Tao, *et al.*, A flexible AMOLED display on the PEN substrate driven by oxide thin-film transistors using anodized aluminium oxide as dielectric, *J. Mater. Chem. C*, 2014, **2**(7), 1255–1259.

95 H. Xu, J. Pang, M. Xu, M. Li, Y. Guo, Z. Chen, *et al.*, Fabrication of flexible amorphous indium-gallium-zinc-oxide thin-film transistors by a chemical vapor deposition-free process on polyethylene napthalate, *ECS J. Solid State Sci. Technol.*, 2014, **3**(9), Q3035–Q3039.

96 J. W. Jo, J. Kim, K. T. Kim, J. G. Kang, M. G. Kim, K. H. Kim, *et al.*, Highly stable and imperceptible electronics utilizing photoactivated heterogeneous sol-gel metal-oxide dielectrics and semiconductors, *Adv. Mater.*, 2015, **27**(7), 1182–1188.

97 G. W. Hyung, J. Park, J. X. Wang, H. W. Lee, Z. H. Li, J. R. Koo, *et al.*, Amorphous indium gallium zinc oxide thin-film transistors with a low-temperature polymeric gate dielectric on a flexible substrate, *Jpn. J. Appl. Phys.*, 2013, **52**(7 PART 1), 071102-4.

98 S. H. Jin, S. K. Kang, I. T. Cho, S. Y. Han, H. U. Chung, D. J. Lee, *et al.*, Water-soluble thin film transistors and circuits based on amorphous indium-gallium-zinc oxide, *ACS Appl. Mater. Interfaces*, 2015, **7**(15), 8268–8274.

99 G. J. Lee, J. Kim, J. H. Kim, S. M. Jeong, J. E. Jang and J. Jeong, High performance, transparent a-IGZO TFTs on a flexible thin glass substrate, *Semicond. Sci. Technol.*, 2014, **29**(3), 035003.

100 Y. Nakajima, M. Nakata, T. Takei, H. Fukagawa, G. Motomura, H. Tsuji, *et al.*, Development of 8-in. oxide-TFT-driven flexible AMOLED display using high-performance red phosphorescent OLED, *J. Soc. Inf. Disp.*, 2014, **22**(3), 137–143.

101 Y. H. Kim, J. S. Heo, T. H. Kim, S. Park, M. H. Yoon, J. Kim, *et al.*, Flexible metal-oxide devices made by room-temperature photochemical activation of sol–gel films, *Nature*, 2012, **489**(7414), 128–132.

102 J. Kim, J. Kim, S. Jo, J. Kang, J. W. Jo, M. Lee, *et al.*, Ultrahigh Detective Heterogeneous Photosensor Arrays with In-Pixel Signal Boosting Capability for Large-Area and Skin-Compatible Electronics, *Adv. Mater.*, 2016, **28**(16), 3078–3086.

103 W. Honda, S. Harada, S. Ishida, T. Arie, S. Akita and K. Takei, High-Performance, Mechanically Flexible, and

Vertically Integrated 3D Carbon Nanotube and InGaZnO Complementary Circuits with a Temperature Sensor, *Adv. Mater.*, 2015, **27**(32), 4674–4680.

104 D. I. Kim, B. U. Hwang, J. S. Park, H. S. Jeon, B. S. Bae, H. J. Lee, *et al.*, Mechanical bending of flexible complementary inverters based on organic and oxide thin film transistors, *Org. Electron.*, 2012, **13**(11), 2401–2405.

105 H. Lai, B. Tzeng, Z. Pei, C. Chen and C. Huang, Ultra-flexible Amorphous Indium-Gallium-Zinc Oxide (a-IGZO), *Thin-Film Transistors*, 2012, (886), 764–767.

106 S. W. Jung, J. S. Choi, J. H. Park, J. B. Koo, C. W. Park, B. S. Na, *et al.*, Oxide semiconductor-based flexible organic/inorganic hybrid thin-film transistors fabricated on polydimethylsiloxane elastomer, *J. Nanosci. Nanotechnol.*, 2016, **16**(3), 2752–2755.

107 M. A. Marrs, C. D. Moyer, E. J. Bawolek, R. J. Cordova, J. Trujillo, G. B. Raupp, *et al.*, Control of threshold voltage and saturation mobility using dual-active-layer device based on amorphous mixed metal-oxide-semiconductor on flexible plastic substrates, *IEEE Trans. Electron Devices*, 2011, **58**(10), 3428–3434.

108 B. S. Yu, J. Y. Jeon, B. C. Kang, W. Lee, Y. H. Kim and T. J. Ha, Wearable 1 V operating thin-film transistors with solution-processed metal-oxide semiconductor and dielectric films fabricated by deep ultra-violet photo annealing at low temperature, *Sci. Rep.*, 2019, **9**(1), 1–13, DOI: 10.1038/s41598-019-44948-z.

109 E. Carlos, J. Leppäniemi, A. Sneck, A. Alastalo, J. Deuermeier, R. Branquinho, *et al.*, Printed, Highly Stable Metal Oxide Thin-Film Transistors with Ultra-Thin High-κ Oxide Dielectric, *Adv. Electron. Mater.*, 2020, **1901071**, 1–10.

110 W.-G. Kim, Y. J. Tak, B. Du Ahn, T. S. Jung, K.-B. Chung and H. J. Kim, High-pressure Gas Activation for Amorphous Indium-Gallium-Zinc-Oxide Thin-Film Transistors at 100 °C, *Sci. Rep.*, 2016, **6**, 23039, DOI: 10.1038/srep23039.

111 Y. S. Rim, H.-W. Choi, K. H. Kim and H. J. Kim, Effects of structural modification via high-pressure annealing on solution-processed InGaO films and thin-film transistors, *J. Phys. D: Appl. Phys.*, 2016, **49**(7), 75112, DOI: 10.1088/0022-3727/49/7/075112.

112 Y. S. Rim, W. H. Jeong, D. L. Kim, H. S. Lim, K. M. Kim and H. J. Kim, Simultaneous modification of pyrolysis and densification for low-temperature solution-processed flexible oxide thin-film transistors, *J. Mater. Chem.*, 2012, **22**(25), 12491–12497, DOI: 10.1039/C2JM16846D.

113 T. Jun, K. Song, Y. Jeong, K. Woo, D. Kim, C. Bae, *et al.*, High-performance low-temperature solution-processable ZnO thin film transistors by microwave-assisted annealing, *J. Mater. Chem.*, 2011, **21**(4), 1102–1108.

114 I. K. Lee, K. H. Lee, S. Lee and W. J. Cho, Microwave annealing effect for highly reliable biosensor: Dual-gate ion-sensitive field-effect transistor using amorphous InGaZnO thin-film transistor, *ACS Appl. Mater. Interfaces*, 2014, **6**(24), 22680–22686.

115 K. W. Jo, S. W. Moon and W. J. Cho, Fabrication of high-performance ultra-thin-body SnO2 thin-film transistors using microwave-irradiation post-deposition annealing, *Appl. Phys. Lett.*, 2015, **106**(4), 043501.

116 J. W. Shin and W. J. Cho, Characteristics of Amorphous In-Ga-Zn-O Thin Films with Various Compositions Under Microwave Annealing, *Phys. Status Solidi A*, 2019, **1900217**, 1–9.

117 K. Gilissen, J. Stryckers, W. Moons, J. Manca and W. Deferme, Microwave annealing, a promising step in the roll-to-roll processing of organic electronics, *Facta. Univ. – Ser Electron. Energy*, 2015, **28**(1), 143–151.

118 Y. J. Lee, B. A. Tsai, T. C. Cho, F. K. Hsueh, P. J. Sung and C. H. Lai, *et al.*, *Low-temperature microwave annealing processes for future IC fabrication*, *2014 IEEE Int Nanoelectron Conf INEC 2014*, 2016, **61**((3)), pp. 651–65.

119 H. C. Cheng and C. Y. Tsay, Flexible a-IZO thin film transistors fabricated by solution processes, *J. Alloys. Compd.*, 2010, **507**(1), L1–L3, DOI: 10.1016/j.jallcom.2010.06.166.

120 S. C. Jang, J. Park, H. D. Kim, H. Hong, K. B. Chung, Y. J. Kim, *et al.*, Low temperature activation of amorphous In-Ga-Zn-O semiconductors using microwave and e-beam radiation, and the associated thin film transistor properties, *AIP Adv.*, 2019, **9**(2), 025204, DOI: 10.1063/1.5082862.

121 R. Xu, J. He, W. Li and D. C. Paine, Performance enhancement of amorphous indium-zinc-oxide thin film transistors by microwave annealing, *Appl. Surf. Sci.*, 2015, **357**, 1915–1919, DOI: 10.1016/j.apsusc.2015.09.135.

122 G. Xia, Q. Zhang and S. Wang, High-Mobility IGZO TFTs by Infrared Radiation Activated Low-Temperature Solution Process, *IEEE Electron Device Lett.*, 2018, **39**(12), 1868–1871.

123 S. Wang, S. Yao, J. Lin and G. Xia, Eco-friendly, low-temperature solution production of oxide thin films for high-performance transistors via infrared irradiation of chloride precursors, *Ceram Int.*, 2019, **45**(8), 9829–9834. Available from: http://www.sciencedirect.com/science/article/pii/S0272884219303086.

124 C.-J. Moon and H.-S. Kim, Intense Pulsed Light Annealing Process of Indium–Gallium–Zinc–Oxide Semiconductors via Flash White Light Combined with Deep-UV and Near-Infrared Drying for High-Performance Thin-Film Transistors, *ACS Appl. Mater. Interfaces*, 2019, **11**(14), 13380–13388, DOI: 10.1021/acsami.8b22458.

125 Y.-H. Kim, J.-S. Heo, T.-H. Kim, S. Park, M.-H. Yoon, J. Kim, *et al.*, Flexible metal-oxide devices made by room-temperature photochemical activation of sol–gel films, *Nature*, 2012, **489**, 128, DOI: 10.1038/nature11434.

126 R. A. John, N. A. Chien, S. Shukla, N. Tiwari, C. Shi, N. G. Ing, *et al.*, Low-temperature chemical transformations for high-performance solution-processed oxide transistors, *Chem. Mater.*, 2016, **28**(22), 8305–8313.

127 K. Tetzner, Y.-H. Lin, A. Regoutz, A. Seitkhan, D. J. Payne and T. D. Anthopoulos, Sub-second photonic processing

of solution-deposited single layer and heterojunction metal oxide thin-film transistors using a high-power xenon flash lamp, *J. Mater. Chem. C*, 2017, **5**(45), 11724–11732, DOI: 10.1039/C7TC03721J.

128 H.-J. Jeong, H.-M. Lee, C.-H. Ryu, E.-J. Park, K.-L. Han, H.-J. Hwang, *et al.*, Ultra-High-Speed Intense Pulsed-Light Irradiation Technique for High-Performance Zinc Oxynitride Thin-Film Transistors, *ACS Appl. Mater. Interfaces*, 2019, **11**(4), 4152–4158, DOI: 10.1021/acsami.8b20291.

129 N. M. Twyman, K. Tetzner, T. D. Anthopoulos, D. J. Payne and A. Regoutz, Rapid photonic curing of solution-processed In2O3 layers on flexible substrates, *Appl. Surf. Sci.*, 2019, **479**, 974–979. Available from: http://www.sciencedirect.com/science/article/pii/S016943321930371X.

130 S. K. Park and Y. H. Kim, Solution-processed metal oxide TFTs and circuits on a plastic by photochemical activation process, *Dig. Tech. Pap. - Soc. Inf. Disp. Int. Symp.*, 2013, **44**(1), 271–274.

131 J. Y. Choi and S. Y. Lee, Comprehensive review on the development of high mobility in oxide thin film transistors, *J. Korean Phys. Soc.*, 2017, **71**(9), 516–527.

132 H. W. Zan, C. C. Yeh, H. F. Meng, C. C. Tsai and L. H. Chen, Achieving high field-effect mobility in amorphous indium-gallium-zinc oxide by capping a strong reduction layer, *Adv. Mater.*, 2012, **24**(26), 3509–3514.

133 Z. Wang, H. A. Al-Jawhari, P. K. Nayak, J. A. Caraveo-Frescas, N. Wei, M. N. Hedhili, *et al.*, Low temperature processed Complementary Metal Oxide Semiconductor (CMOS) device by oxidation effect from capping layer, *Sci. Rep.*, 2015, **5**, 1–6.

134 Y. Shin, S. T. Kim, K. Kim, M. Y. Kim, S. Oh and J. K. Jeong, The Mobility Enhancement of Indium Gallium Zinc Oxide Transistors via Low-temperature Crystallization using a Tantalum Catalytic Layer, *Sci. Rep.*, 2017, **7**(1), 1–10.

135 T. Kim, M. J. Kim, J. Lee and J. K. Jeong, Boosting Carrier Mobility in Zinc Oxynitride Thin-Film Transistors via Tantalum Oxide Encapsulation, *ACS Appl. Mater. Interfaces*, 2019, **11**(25), 22501–22509.

136 K. T. Kim, J. Kim, Y. H. Kim and S. K. Park, In-situ metallic oxide capping for high mobility solution-processed metal-oxide TFTs, *IEEE Electron Device Lett.*, 2014, **35**(8), 850–852.

137 M. R. Kulkarni, R. A. John, N. Tiwari, A. Nirmal, S. E. Ng, A. C. Nguyen, *et al.*, Field-Driven Athermal Activation of Amorphous Metal Oxide Semiconductors for Flexible Programmable Logic Circuits and Neuromorphic Electronics, *Small*, 2019, **1901457**, 1–11.

138 P. R. Pudasaini, J. H. Noh, A. T. Wong, O. S. Ovchinnikova, A. V. Haglund, S. Dai, T. Z. Ward, D. Mandrus and P. D. Rack, Ionic Liquid Activation of Amorphous Metal-Oxide Semiconductors for Flexible Transparent Electronic Devices, *Adv. Funct. Mater.*, 2016, **26**, 2820–2825.

139 J. Jeong, N. Aetukuri, T. Graf, T. D. Schaldt, M. G. Samant and S. S. S. Parkin, Suppression of Metal-Insulator Transition in VO2 by Electric Field–Induced Oxygen Vacancy Formation, *Science*, 2013, **339**(March), 1402–1406.

140 K. Ueno, S. Nakamura, H. Shimotani, H. T. Yuan, N. Kimura, T. Nojima, *et al.*, Discovery of superconductivity in KTaO 3 by electrostatic carrier doping, *Nat. Nanotechnol.*, 2011, **6**(7), 408–412.

141 J. T. Yang, C. Ge, J. Y. Du, H. Y. Huang, M. He, C. Wang, *et al.*, Artificial synapses emulated by an electrolyte-gated tungsten-oxide transistor, *Adv. Mater.*, 2018, **30**(34), 1–10.

142 E. Bacaksiz, M. Parlak, M. Tomakin, A. Özçelik, M. Karakız and M. Altunbaş, The effects of zinc nitrate, zinc acetate and zinc chloride precursors on investigation of structural and optical properties of ZnO thin films, *J. Alloys Compd.*, 2008, **466**(1), 447–450. Available from: http://www.sciencedirect.com/science/article/pii/S0925838807021998.

143 K.-H. Lim, J. Lee, J.-E. Huh, J. Park, J.-H. Lee, S.-E. Lee, *et al.*, A systematic study on effects of precursors and solvents for optimization of solution-processed oxide semiconductor thin-film transistors, *J. Mater. Chem. C*, 2017, **5**(31), 7768–7776, DOI: 10.1039/C7TC01779K.

144 W. H. Jeong, J. H. Bae and H. J. Kim, High-Performance Oxide Thin-Film Transistors Using a Volatile Nitrate Precursor for Low-Temperature Solution Process, *IEEE Electron Device Lett.*, 2012, **33**(1), 68–70.

145 K. K. Banger, Y. Yamashita, K. Mori, R. L. Peterson, T. Leedham, J. Rickard, *et al.*, Low-temperature, high-performance solution-processed metal oxide thin-film transistors formed by a 'sol–gel on chip' process, *Nat. Mater.*, 2010, **10**, 45, DOI: 10.1038/nmat2914.

146 S. T. Meyers, J. T. Anderson, C. M. Hung, J. Thompson, J. F. Wager and D. A. Keszler, Aqueous Inorganic Inks for Low-Temperature Fabrication of ZnO TFTs, *J. Am. Chem. Soc.*, 2008, **130**(51), 17603–17609, DOI: 10.1021/ja808243k.

147 Y. Hwan Hwang, J.-S. Seo, J. Moon Yun, H. Park, S. Yang, S.-H. Ko Park, *et al.*, An 'aqueous route' for the fabrication of low-temperature-processable oxide flexible transparent thin-film transistors on plastic substrates, *NPG Asia Mater.*, 2013, **5**, e45–e45, DOI: 10.1038/am.2013.11.

148 Y. S. Rim, H. Chen, T.-B. Song, S.-H. Bae and Y. Yang, Hexaaqua Metal Complexes for Low-Temperature Formation of Fully Metal Oxide Thin-Film Transistors, *Chem. Mater.*, 2015, **27**(16), 5808–5812, DOI: 10.1021/acs.chemmater.5b02505.

149 M.-G. Kim, M. G. Kanatzidis, A. Facchetti and T. J. Marks, Low-temperature fabrication of high-performance metal oxide thin-film electronics via combustion processing, *Nat. Mater.*, 2011, **10**, 382, DOI: 10.1038/nmat3011.

150 E. A. Cochran, D.-H. Park, M. G. Kast, L. J. Enman, C. K. Perkins, R. H. Mansergh, *et al.*, Role of Combustion Chemistry in Low-Temperature Deposition of Metal Oxide Thin Films from Solution, *Chem. Mater.*, 2017, **29**(21), 9480–9488, DOI: 10.1021/acs.chemmater.7b03618.

151 S. J. Kim, A. R. Song, S. S. Lee, S. Nahm, Y. Choi, K.-B. Chung, *et al.*, Independent chemical/physical role of

combustive exothermic heat in solution-processed metal oxide semiconductors for thin-film transistors, *J. Mater. Chem. C*, 2015, **3**(7), 1457–1462, DOI: 10.1039/C4TC02408G.

152 J. W. Hennek, M.-G. Kim, M. G. Kanatzidis, A. Facchetti and T. J. Marks, Exploratory Combustion Synthesis: Amorphous Indium Yttrium Oxide for Thin-Film Transistors, *J. Am. Chem. Soc.*, 2012, **134**(23), 9593–9596, DOI: 10.1021/ja303589v.

153 Y. H. Kang, K.-S. Jang, C. Lee and S. Y. Cho, Facile Preparation of Highly Conductive Metal Oxides by Self-Combustion for Solution-Processed Thermoelectric Generators, *ACS Appl. Mater. Interfaces*, 2016, **8**(8), 5216–5223, DOI: 10.1021/acsami.5b10187.

154 Y. Chen, B. Wang, W. Huang, X. Zhang, G. Wang, M. J. Leonardi, *et al.*, Nitroacetylacetone as a Cofuel for the Combustion Synthesis of High-Performance Indium–Gallium–Zinc Oxide Transistors, *Chem. Mater.*, 2018, **30**(10), 3323–3329, DOI: 10.1021/acs.chemmater.8b00663.

155 B. Wang, L. Zeng, W. Huang, F. S. Melkonyan, W. C. Sheets, L. Chi, *et al.*, Carbohydrate-Assisted Combustion Synthesis To Realize High-Performance Oxide Transistors, *J. Am. Chem. Soc.*, 2016, **138**(22), 7067–7074, DOI: 10.1021/jacs.6b02309.

156 Y. H. Kang, S. Jeong, J. M. Ko, J.-Y. Lee, Y. Choi, C. Lee, *et al.*, Two-component solution processing of oxide semiconductors for thin-film transistors via self-combustion reaction, *J. Mater. Chem. C*, 2014, **2**(21), 4247–4256, DOI: 10.1039/C4TC00139G.

157 X. Liang, C. Wang, J. Liang, C. Liu and Y. Pei, Efficient Defect Engineering for Solution Combustion Processed In-Zn-O thin films for high performance transistors, *Semicond. Sci. Technol.*, 2017, **32**(9), 095010.

158 K. Takenaka, M. Endo, G. Uchida and Y. Setsuhara, Fabrication of high-performance InGaZnOx thin film transistors based on control of oxidation using a low-temperature plasma, *Appl. Phys. Lett.*, 2018, **112**(15), 152103, DOI: 10.1063/1.5011268.

159 E. Lee, T. Kim, A. Benayad, H. Kim, S. Jeon and G.-S. Park, Ar plasma treated ZnON transistor for future thin film electronics, *Appl. Phys. Lett.*, 2015, **107**(12), 122105, DOI: 10.1063/1.4930827.

160 M. Miyakawa, M. Nakata, H. Tsuji and Y. Fujisaki, (Invited) Fabrication Technique for Low-Temperature Aqueous Solution-Processed Oxide Thin-Film Transistors, *ECS Trans.*, 2018, **86**(11), 105–109. Available from: http://ecst.ecsdl.org/content/86/11/105.abstract.

161 X. Li, J. Cheng, Y. Chen, Y. He, Y. Li, J. Xue, *et al.*, Low-Temperature Aqueous Route Processed Indium Oxide Thin-Film Transistors by NH3 Plasma-Assisted Treatment, *IEEE Trans. Electron Devices*, 2019, **66**(3), 1302–1307.

162 J. Cheng, Z. Yu, X. Li, J. Guo, W. Yan, J. Xue, *et al.*, The Effects of N2O Plasma Treatment on the Device Performance of Solution-Processed a-InMgZnO Thin-Film Transistors, *IEEE Trans. Electron Devices*, 2018, **65**(1), 136–141.

163 W.-T. Park, I. Son, H.-W. Park, K.-B. Chung, Y. Xu, T. Lee, *et al.*, Facile Routes To Improve Performance of Solution-Processed Amorphous Metal Oxide Thin Film Transistors by Water Vapor Annealing, *ACS Appl. Mater. Interfaces*, 2015, **7**(24), 13289–13294, DOI: 10.1021/acsami.5b04374.

164 J. K. Kang, S. P. Park, J. W. Na, J. H. Lee, D. Kim and H. J. Kim, Improvement in Electrical Characteristics of Eco-friendly Indium Zinc Oxide Thin-Film Transistors by Photocatalytic Reaction, *ACS Appl. Mater. Interfaces*, 2018, **10**(22), 18837–18844.

165 J. Cheng, X. Li, J. Guo, H. Xu, Y. Chen, Y. He, *et al.*, The role of the sequence of plasma treatment and high temperature annealing on solution-processed a-IMZO thin film transistor, *J. Alloys Compd.*, 2019, **793**, 369–374. Available from: http://www.sciencedirect.com/science/article/pii/S0925838819313945.

166 J. Park, J.-E. Huh, S.-E. Lee, J. Lee, W. H. Lee, K.-H. Lim, *et al.*, Effective Atmospheric-Pressure Plasma Treatment toward High-Performance Solution-Processed Oxide Thin-Film Transistors, *ACS Appl. Mater. Interfaces*, 2018, **10**(36), 30581–30586, DOI: 10.1021/acsami.8b11111.

167 Y.-H. Hwang, K.-S. Kim and W.-J. Cho, Effects of combined Ar/O2plasma and microwave irradiation on electrical performance and stability in solution-deposited amorphous InGaZnO thin-film transistors, *Jpn. J. Appl. Phys.*, 2014, **53**(4S), 04EF12–04EF12, DOI: 10.7567/JJAP.53.04EF12.

168 I. Bretos, R. Jiménez, J. Ricote and M. L. Calzada, Low-temperature crystallization of solution-derived metal oxide thin films assisted by chemical processes, *Chem. Soc. Rev.*, 2018, **47**(2), 291–308, DOI: 10.1039/C6CS00917D.

169 L. F. Teng, P. T. Liu, Y. J. Lo and Y. J. Lee, Effects of microwave annealing on electrical enhancement of amorphous oxide semiconductor thin film transistor, *Appl. Phys. Lett.*, 2012, **101**(13), 1–5.

